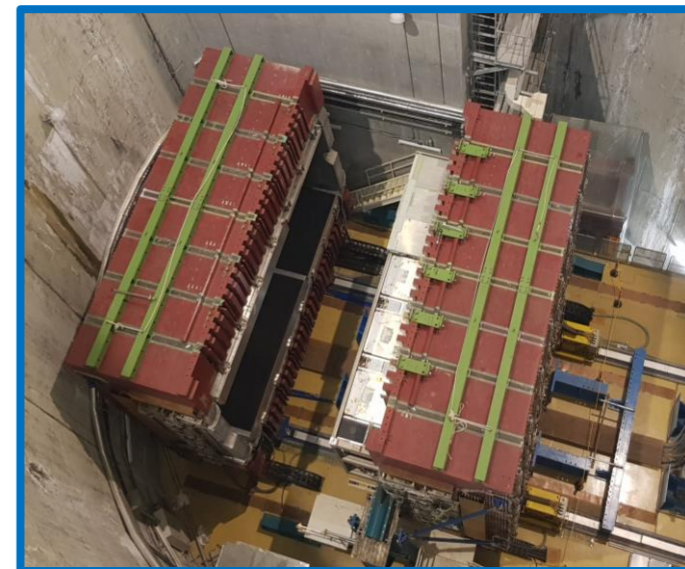


Study of charged current interactions on carbon with a single positively charged pion in the final state at the T2K off-axis near detector with 4π solid angle acceptance

Danaisis Vargas Oliva
 University of Toronto
danaisis.vargas@cern.ch

October 28th, 2022

Hoam Faculty House at Seoul National University, Seoul, KOREA
<https://nuint22.org>



On top of ND280



Inside Super-Kamiokande

The T2K experiment and motivation

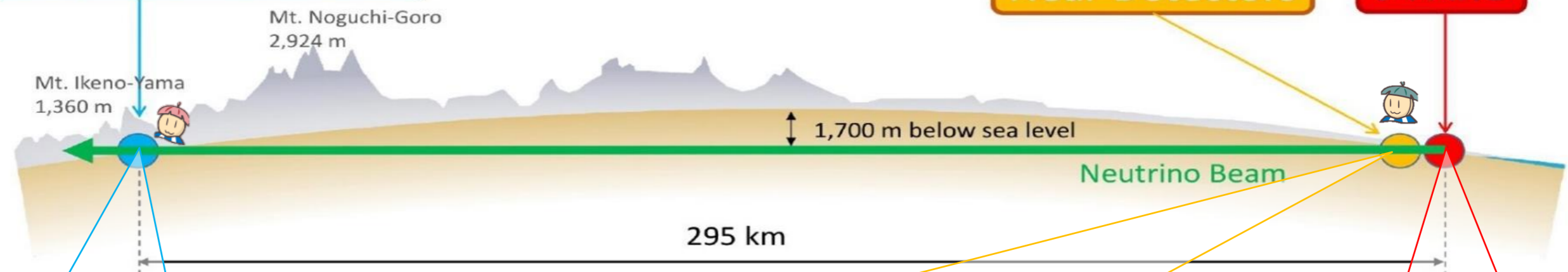
T2K Measures neutrino oscillations
 $\bar{\nu}_\mu/\nu_\mu$ disappearance and $\bar{\nu}_e/\nu_e$ appearance, the oscillation
parameters θ_{13} , θ_{23} , and δ_{CP} .

T2K is sensitive to the mass hierarchy (Δm_{32}^2) through
matter effect.

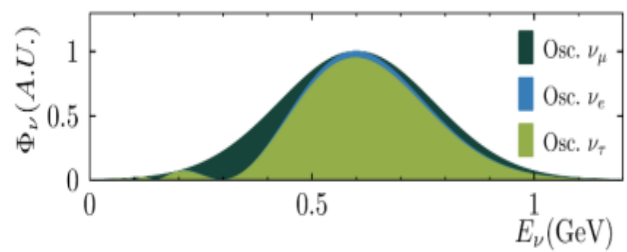
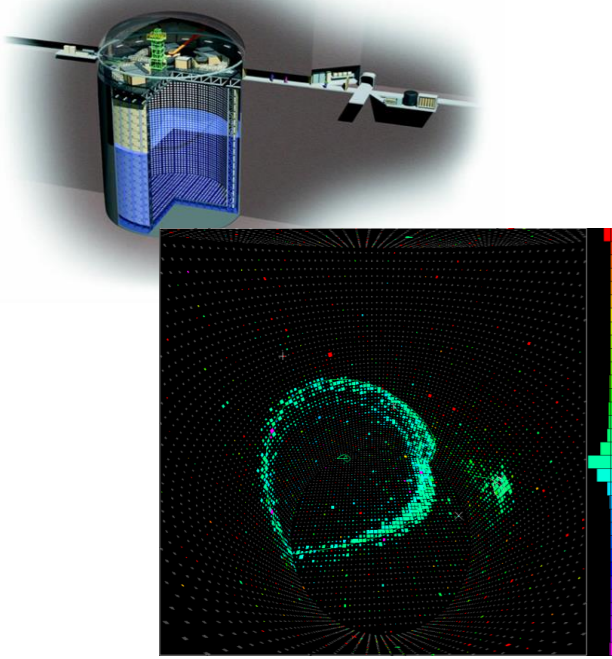
Super-Kamiokande

Near Detectors

J-PARC

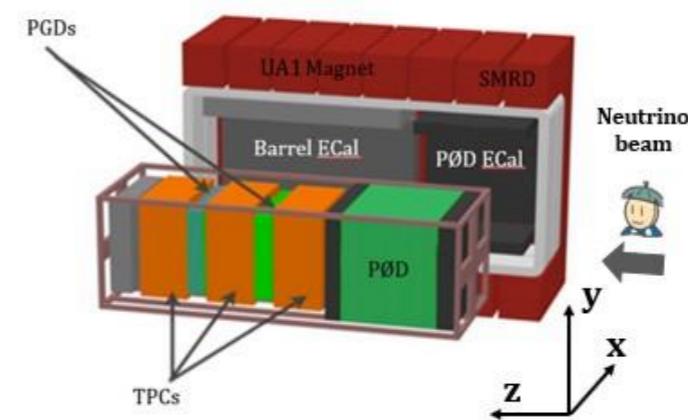
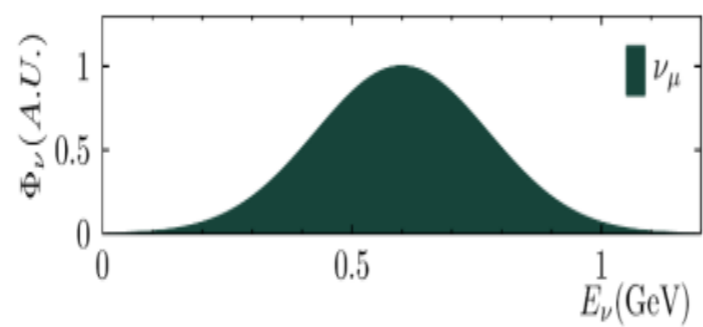


Measure oscillated spectrum

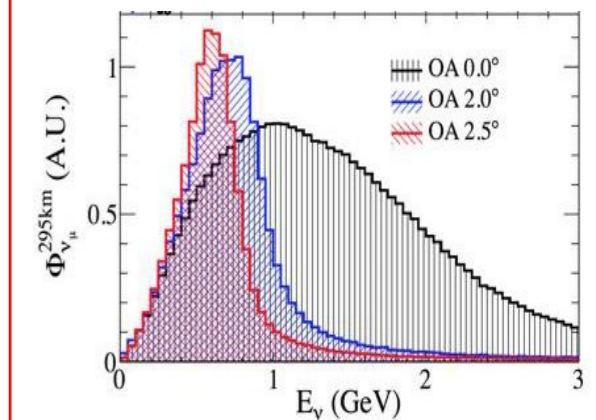
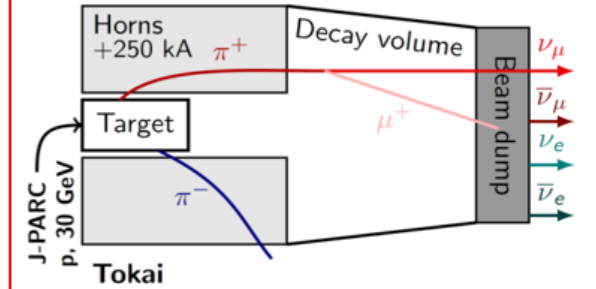


Measure un-oscillated spectrum

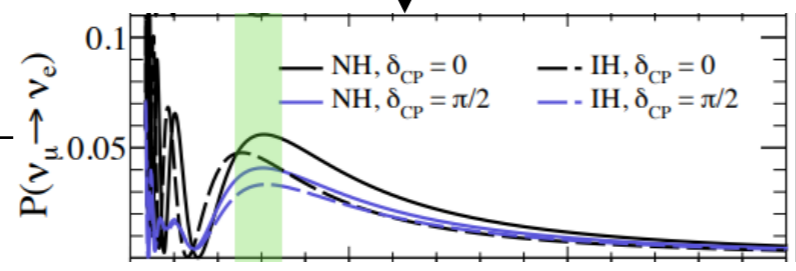
Are used to constrain the flux and cross section parameters reducing the systematics errors in the T2K oscillation analyses.



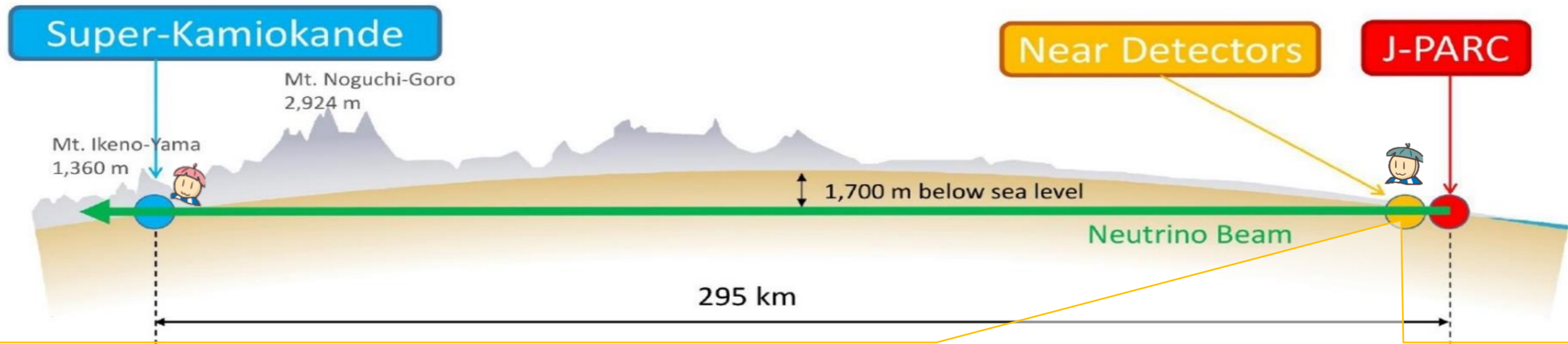
Measure flux spectrum



$$N_x(E_\nu) = \underbrace{\phi(E_\nu) \sigma(E_\nu) \epsilon(E_\nu)}_{\text{Near detector}} \underbrace{P(\nu_\mu \rightarrow \nu_x)}_{\text{Far detector}}$$

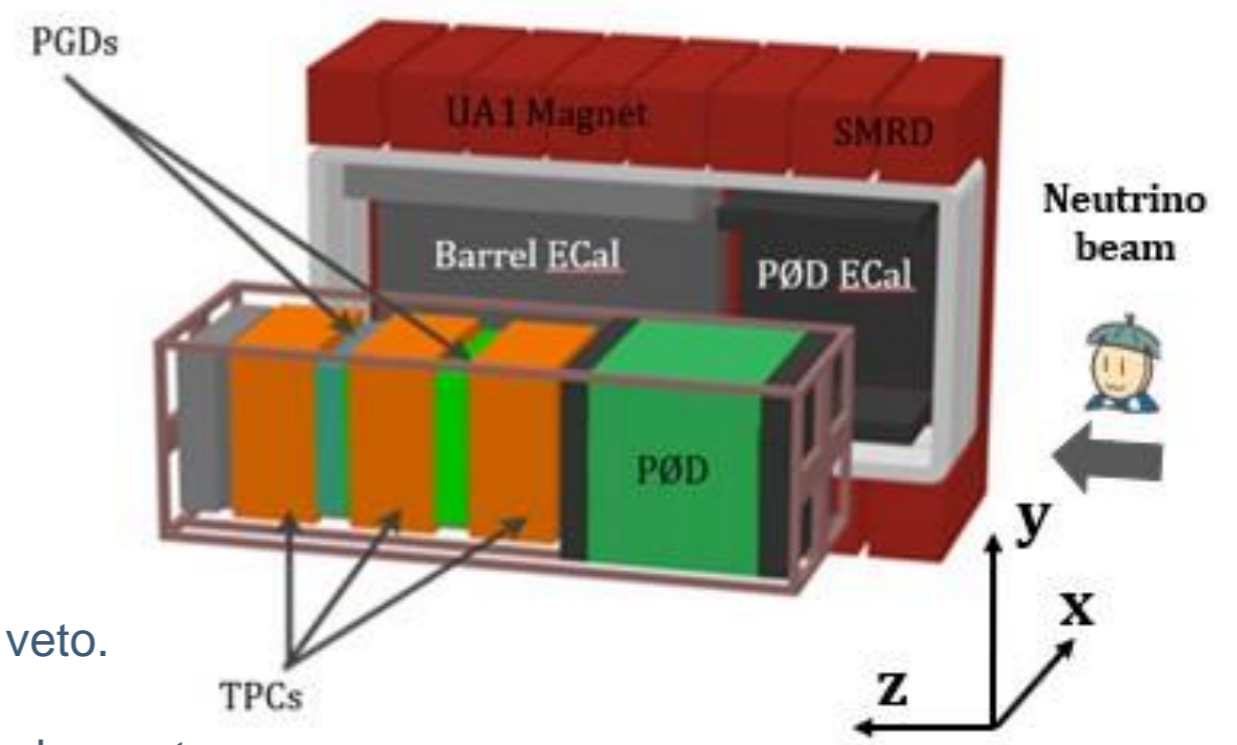


Talks from: C.J. Valls C.Wret, S.Dolan, L. Munteanu, and C. Schloesser.



Off-axis (2.5 degrees) ND280

- π^0 Detector (P \emptyset D): neutral pion detector, optimized for NC interactions.
- Time Projection Chambers (TPCs): energy, angle and identification
- Fine grained detector (FGDs): active target
 - **FGD1: Hydrocarbon** and FGD2: Hydrocarbon + Water
- Electromagnetic Calorimeters (ECals): separate tracks from showers and as veto.
- Side Muon Range Detector (SMRD): energy of muons based on the range and as veto.
- Magnet: charge of the particles and momentum.



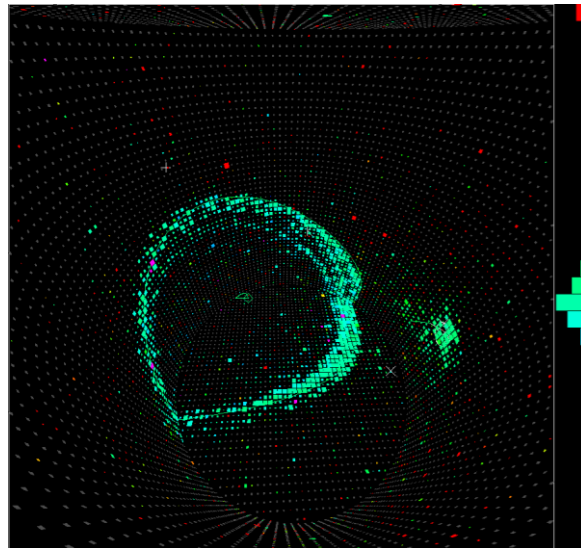
Why we look at ND280 4π solid angle acceptance?

Different flux, target and solid angle acceptance.

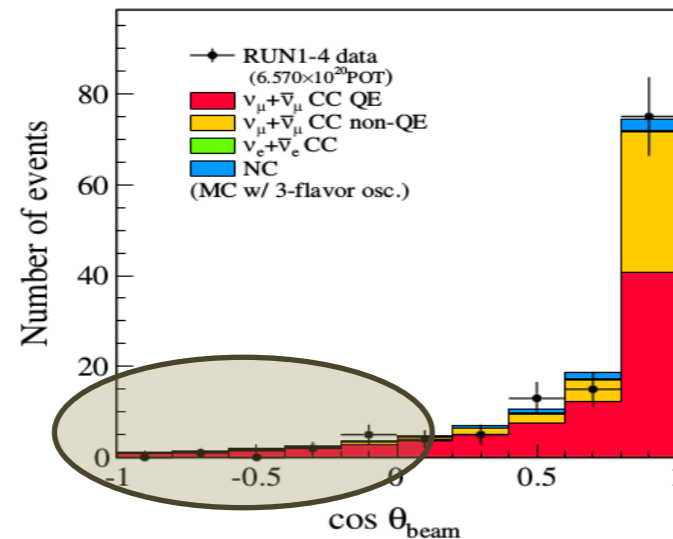
Near/far detector ratios don't fully cancel systematics:

- Different near/far detector design acceptance.

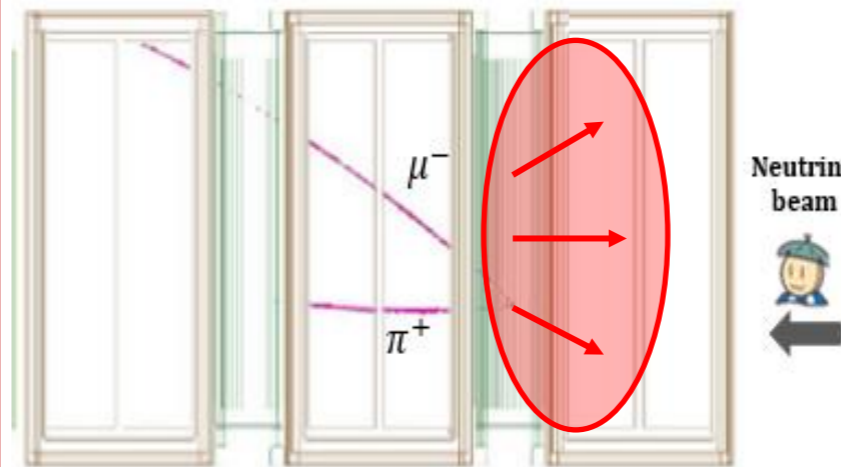
SK detector
↓
 4π acceptance



The $\cos \theta_{\text{beam}}$ distribution in the events selected for the ν_{μ} disappearance analysis at SK

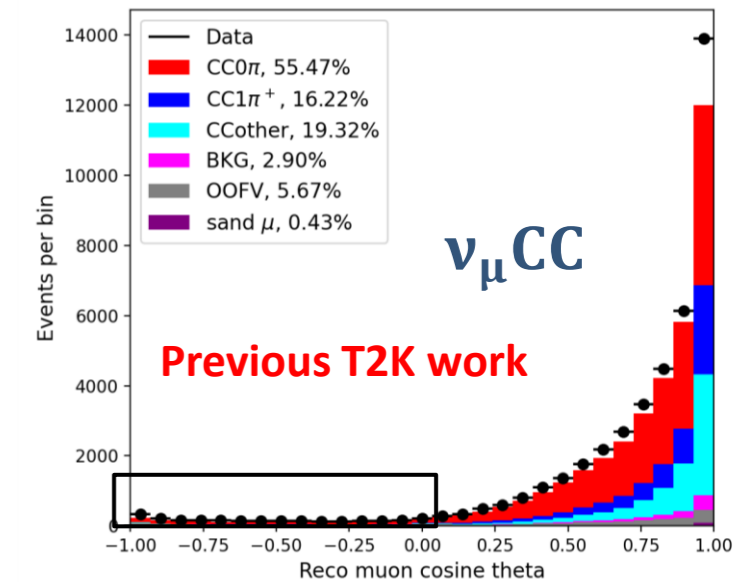
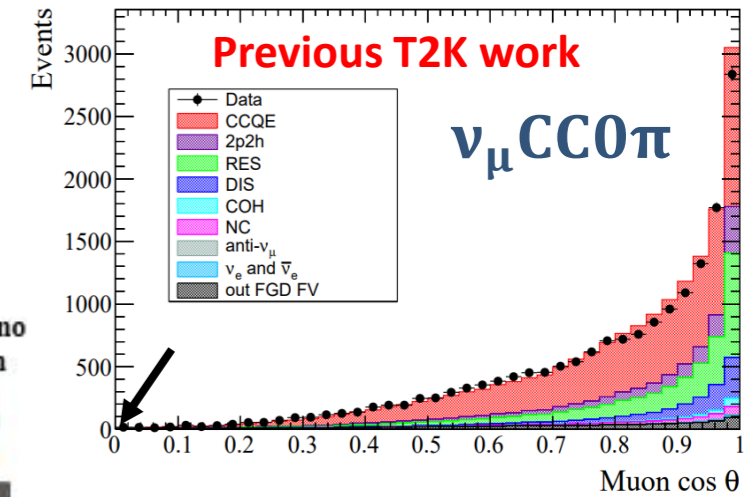


ND280
↓
Forward-going tracks



ND280
↓
 4π acceptance

The $\cos \theta_{\mu}$ distribution



Why measure the ν_μ CC1 π^+ cross-section?

Neutrino oscillation parameters require a precise knowledge of the interaction cross section and the systematic errors are currently dominated by cross section and flux uncertainties.

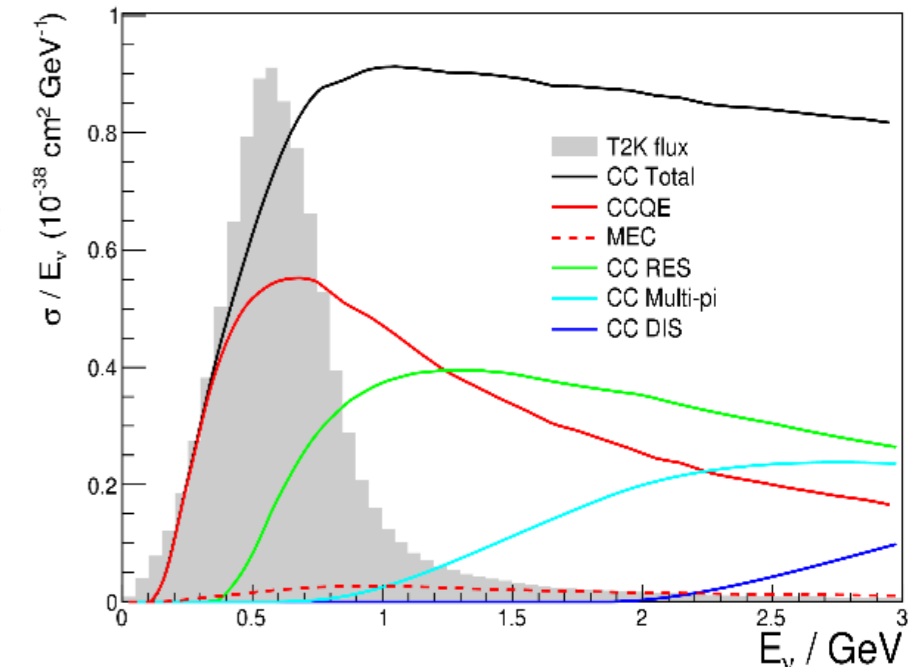
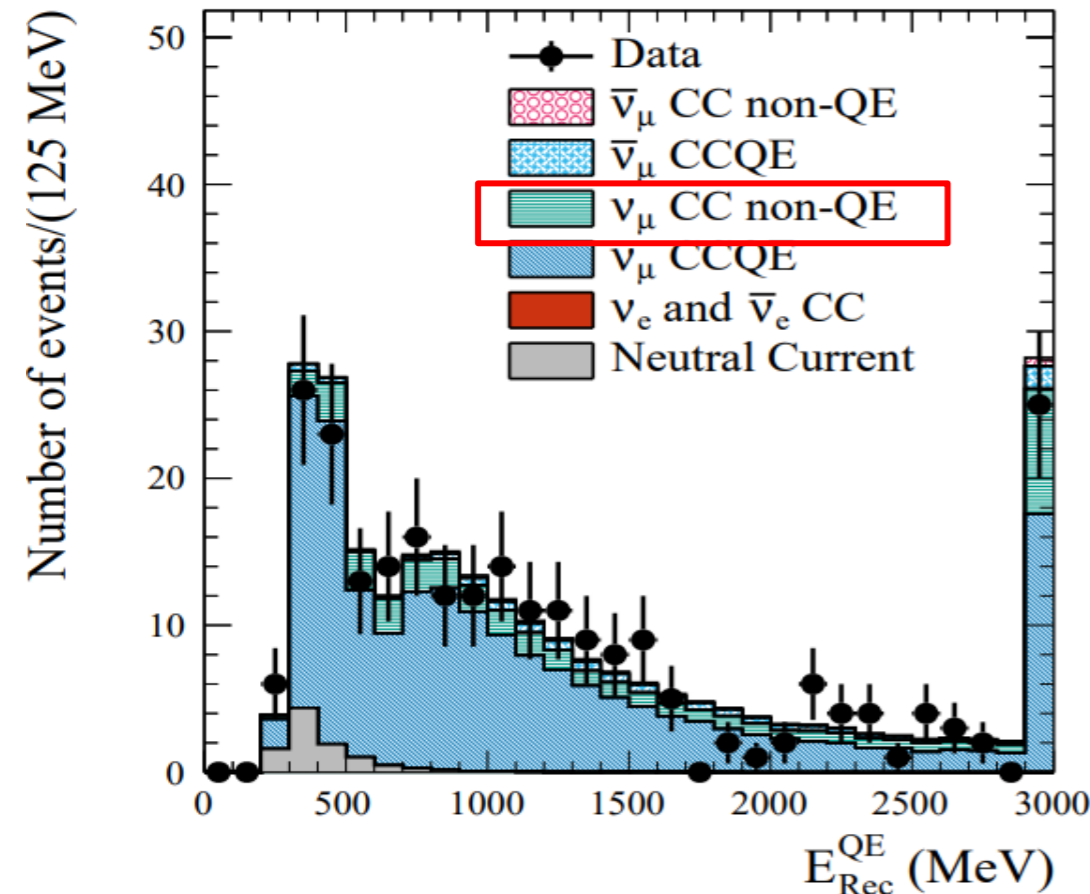
- Cross sections are used to:
 - understand how neutrinos interact with matter.
 - control the bias on the reconstructed energy
 - reduce uncertainties on the event rate at Super-Kamiokande.

Error source	1-Ring μ	
	FHC	RHC
SK Detector	2.4	2.0
SK FSI+SI+PN	2.2	2.0
Flux + Xsec (ND unconstrained)	14.3	11.8
Flux + Xsec (ND constrained)	3.3	2.9
Nucleon Removal Energy	2.4	1.7
$\sigma(\nu_e)/\sigma(\bar{\nu}_e)$	0.0	0.0
NC1 γ	0.0	0.0
NC Other	0.3	0.3
$\sin^2 \theta_{23} + \Delta m_{21}^2$	0.0	0.0
$\sin^2 \theta_{13}$ PDG2018	0.0	0.0
All Systematics	5.1	4.5

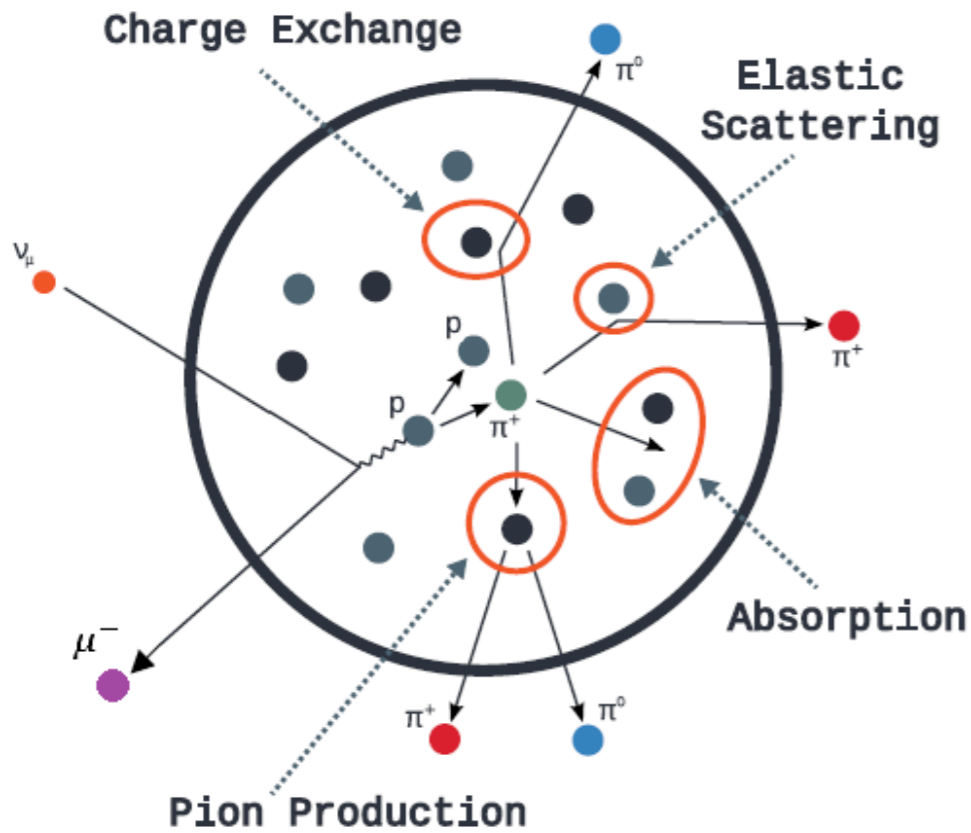
- ν_μ CC1 π^+ events constitute the main background for the ν_μ disappearance measurement.
- CC1 π^+ events (2 rings) is a new signal at SK.
- Pion production is dominated by resonant interactions in the T2K energy range.

Single pion production issues

- Missing models of nuclear effects.
- No consistent way to model RES/DIS transition.



Neutrino-nucleus interactions



As consequence, the kinematics and/or **interaction topology** can be altered.

$$\text{CCQE: } \nu_\mu + n \rightarrow \mu^- + p$$

$$\text{CCRES: } \nu_\mu + p \rightarrow \mu^- + p + \pi^+$$

$$\nu_\mu + n \rightarrow \mu^- + n + \pi^+$$

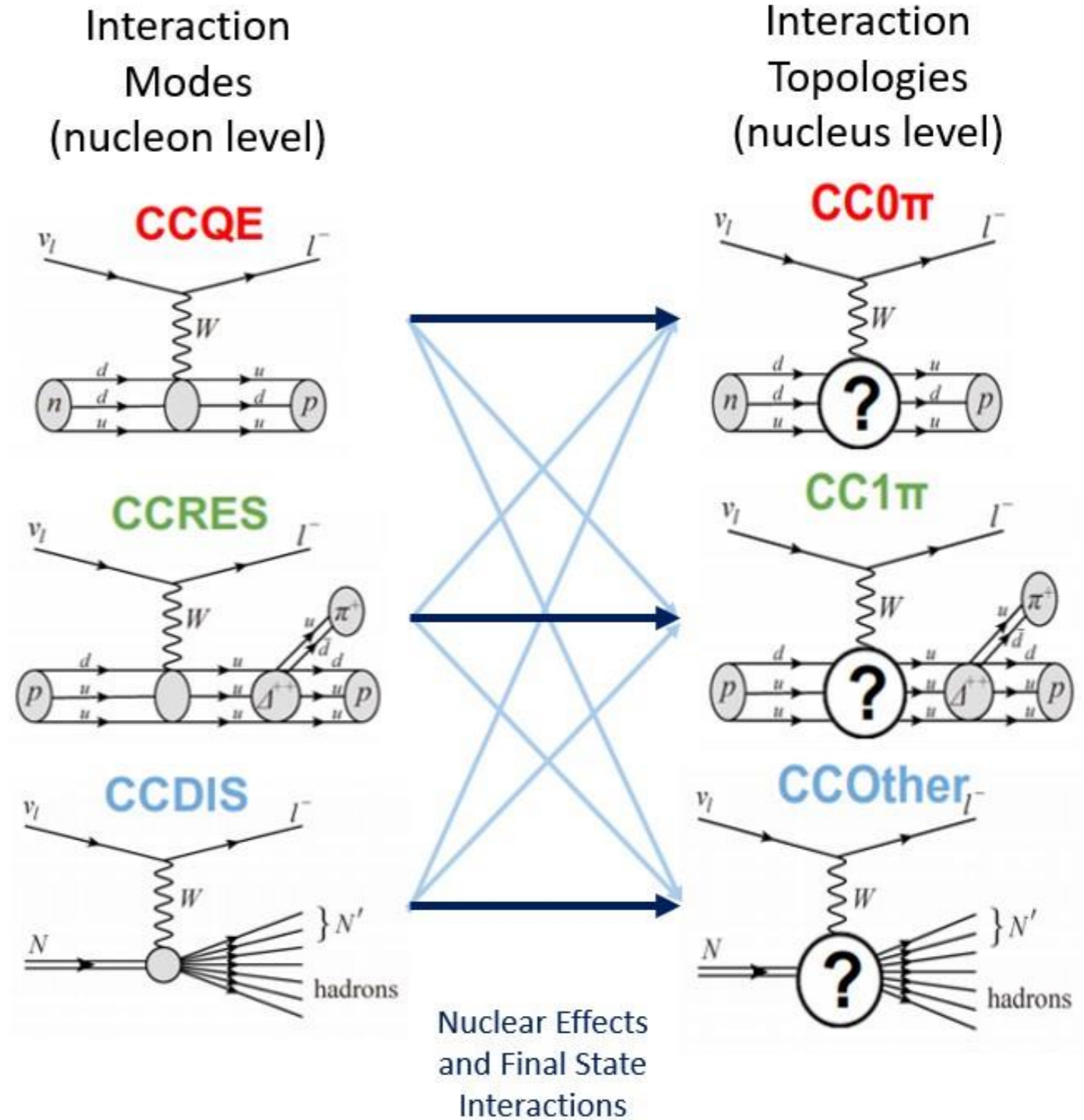


Figure from Dr. Stephen Dolan

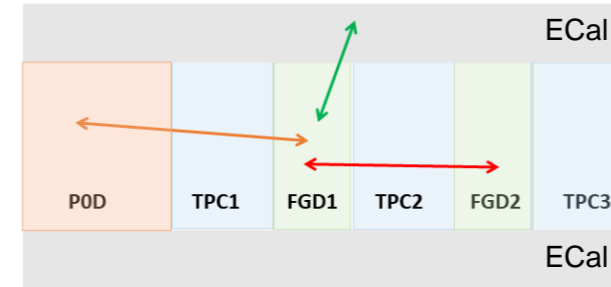
Selection

Selection steps

ND280
Events

general event quality
multiplicity
time of flight
fiducial volume

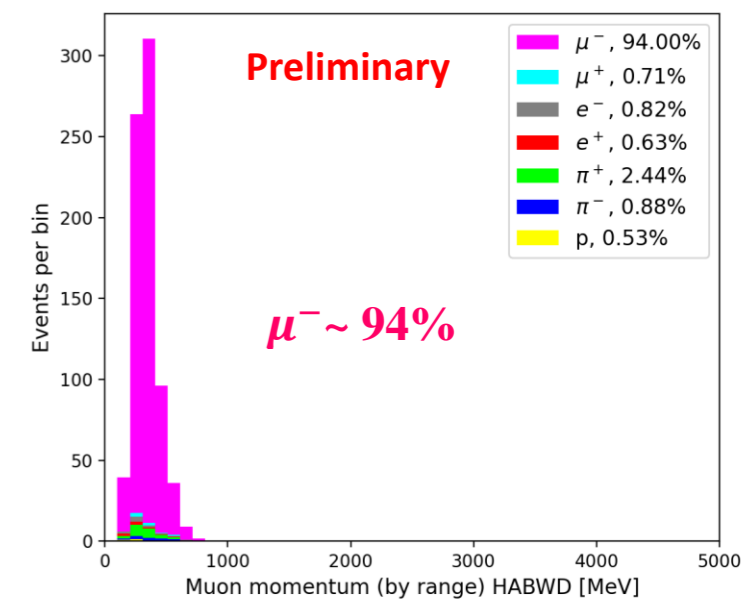
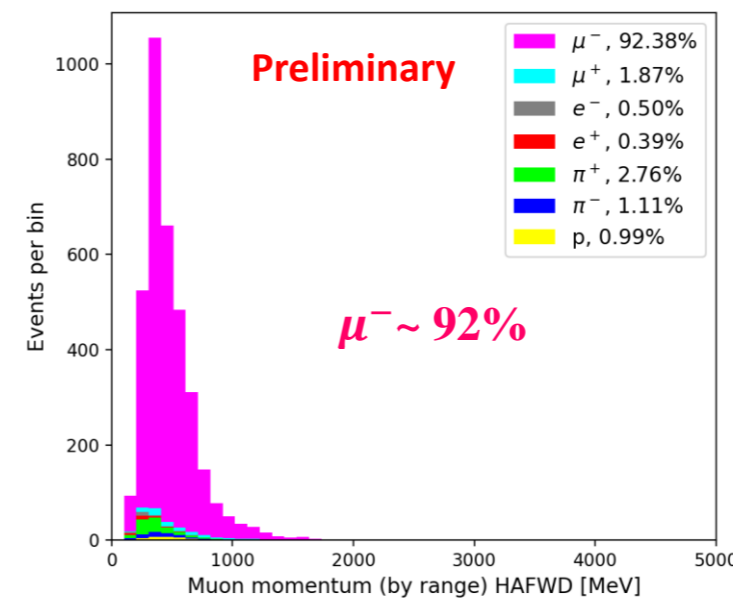
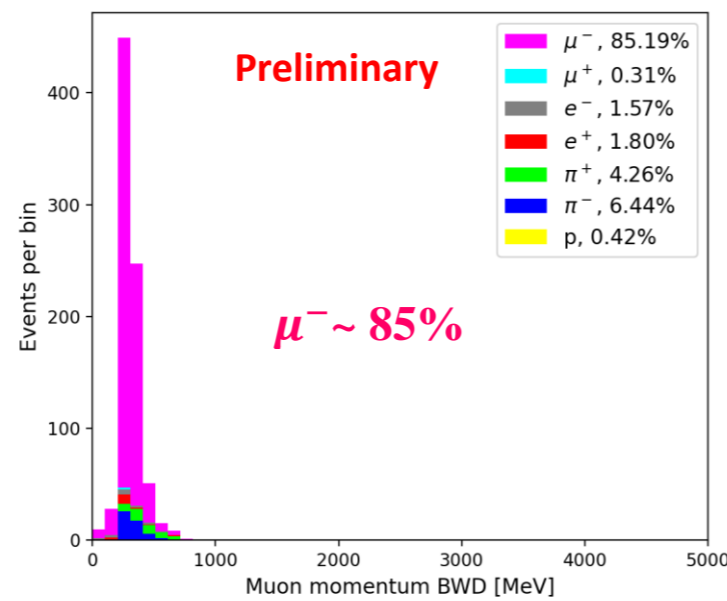
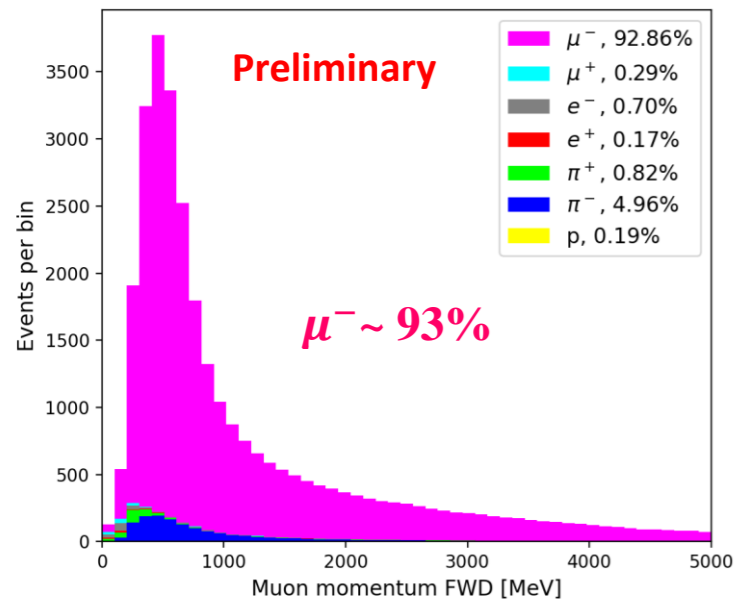
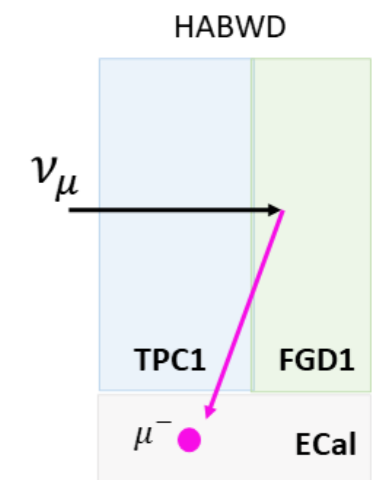
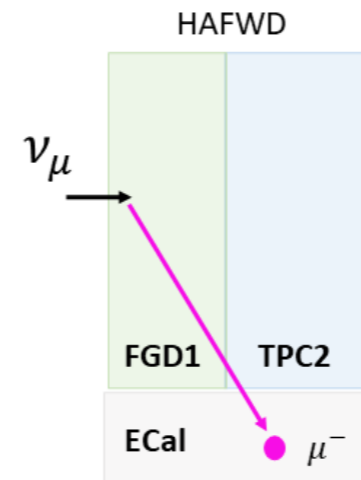
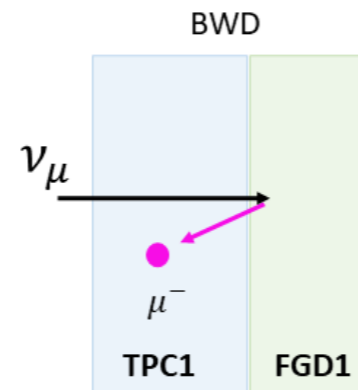
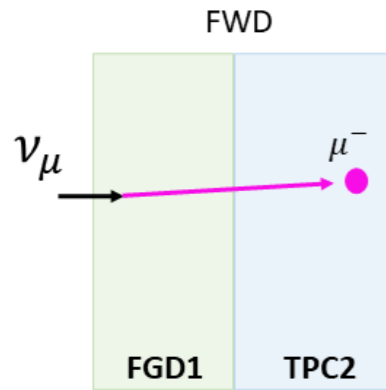
direction of the main track
apply PID for muons



$$ToF_{POD-FGD1} = t_{FGD1} - t_{POD}$$

$$ToF_{ECal-FGD1} = t_{FGD1} - t_{BrECal}$$

$$ToF_{FGD1-FGD2} = t_{FGD2} - t_{FGD1}$$



Selection steps

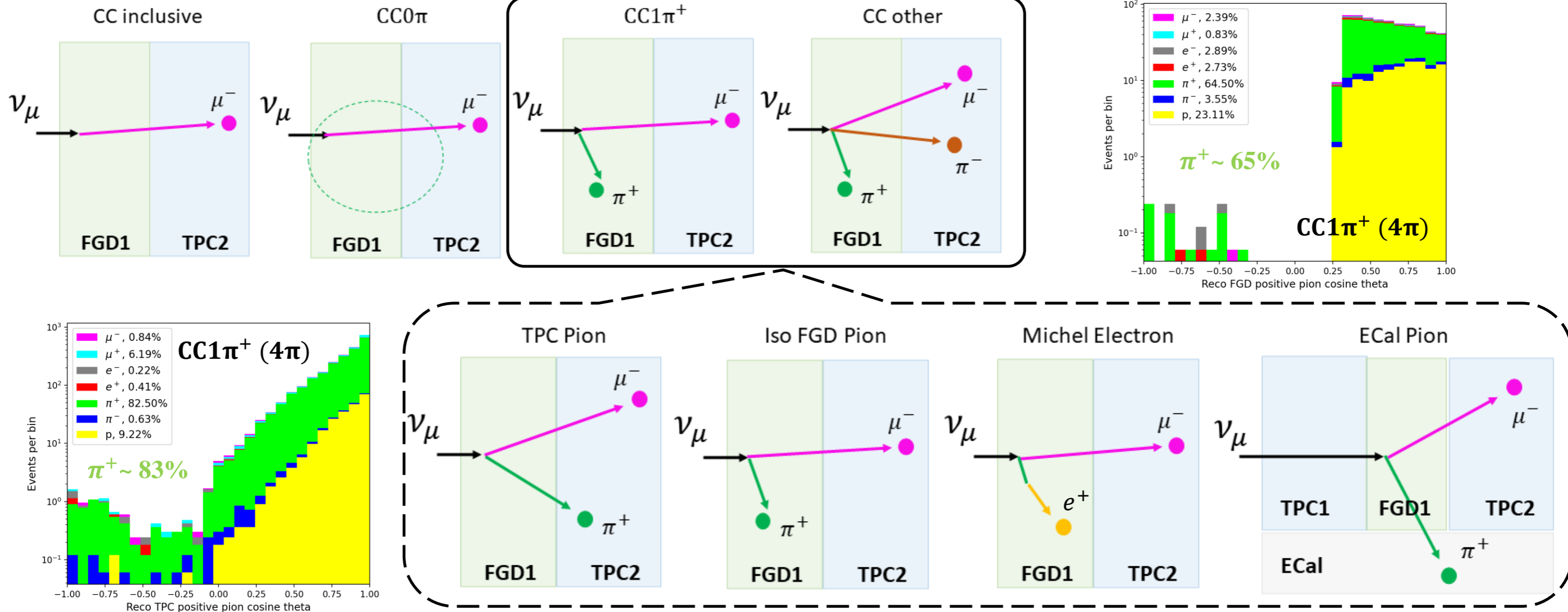
ND280 Events

general event quality
multiplicity
time of flight
fiducial volume

direction of the main track
apply PID for muons

Pion multiplicity

Additional steps for improving the purity of the samples

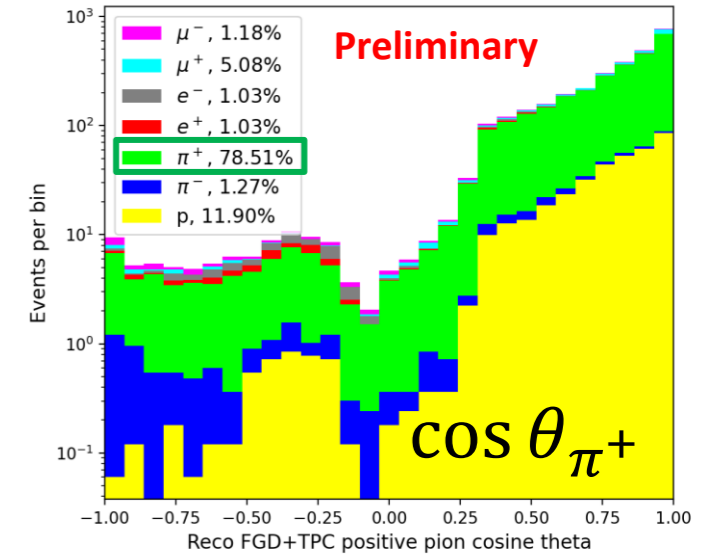
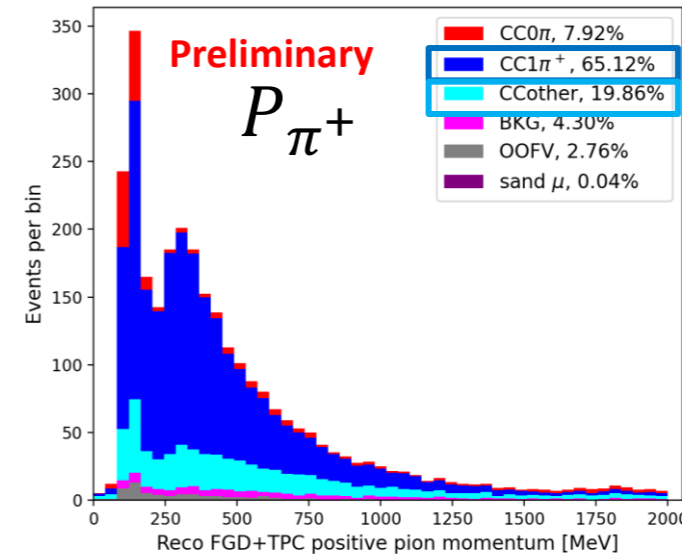
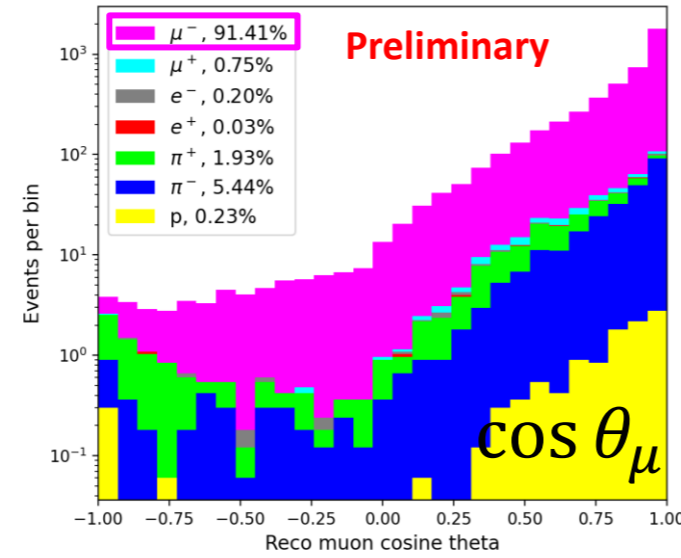
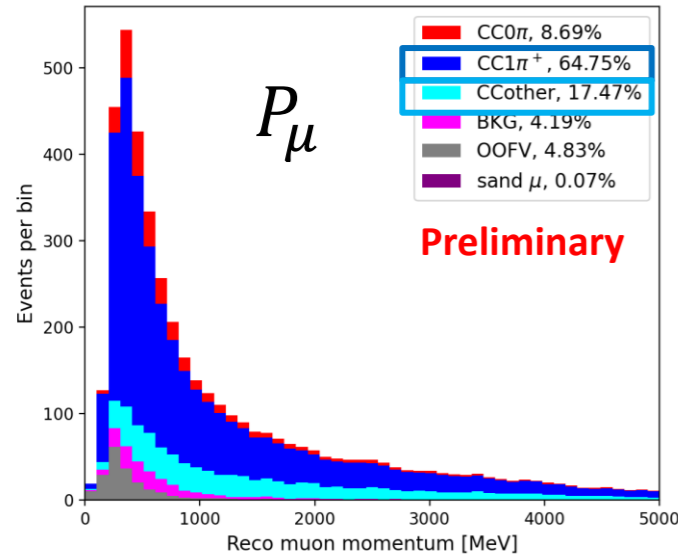


Performance: CC1 π^+ signal

Muon

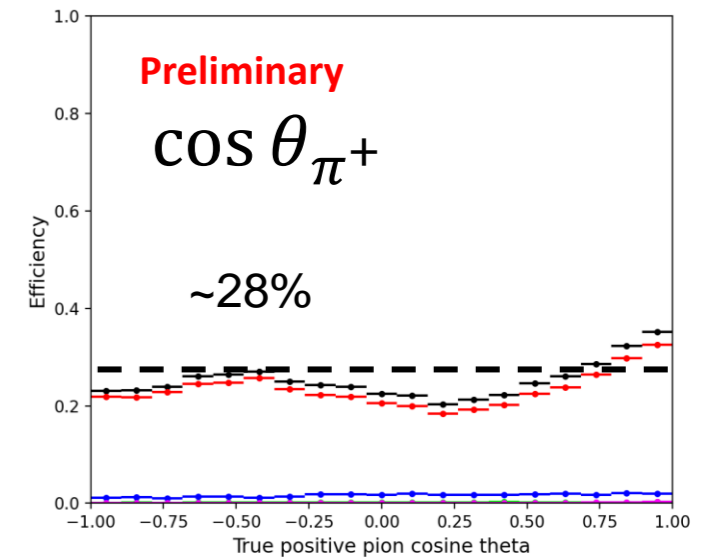
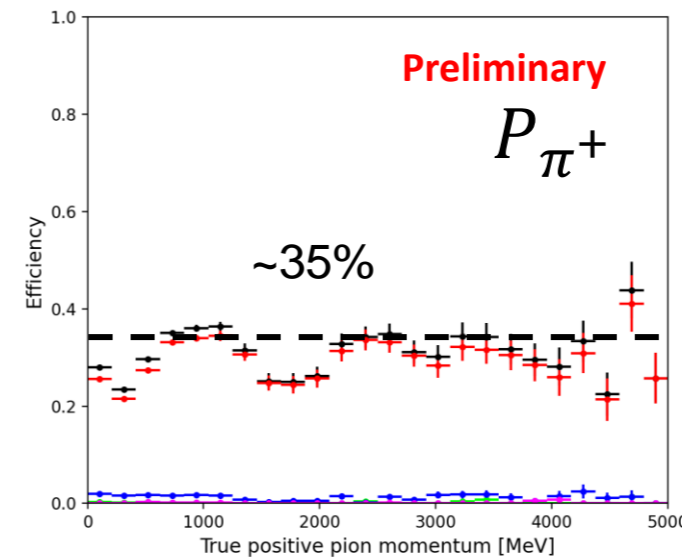
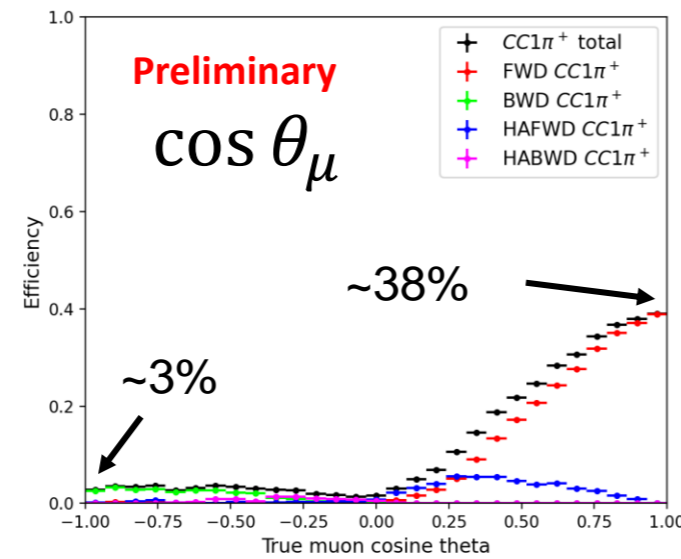
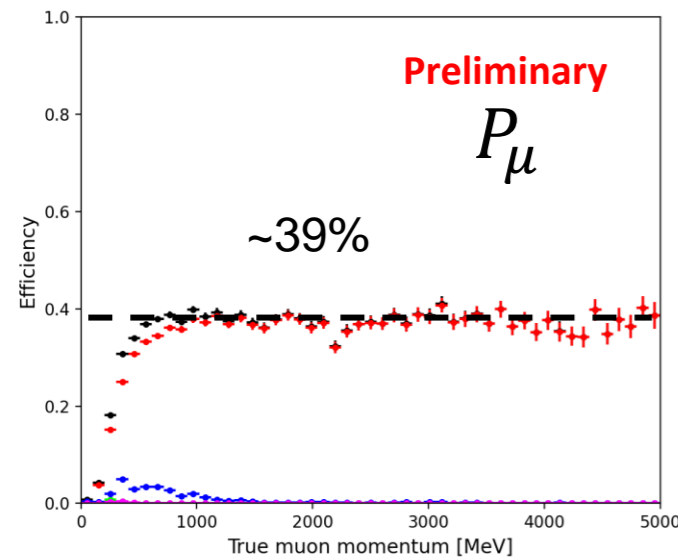
Positive pion

purity



Muon momentum, muon cosine of theta, positive pion momentum, and positive pion cosine of theta distributions with 4 π solid angle acceptance. Using the true topology and particle definition.

efficiency



Efficiency of CC1 π^+ vs. muon momentum, muon cosine of theta, positive pion momentum, and positive pion cosine of theta respectively.

Analysis overview

Signal definition

Target:

- Hydrocarbon (C_8H_8) \rightarrow carbon

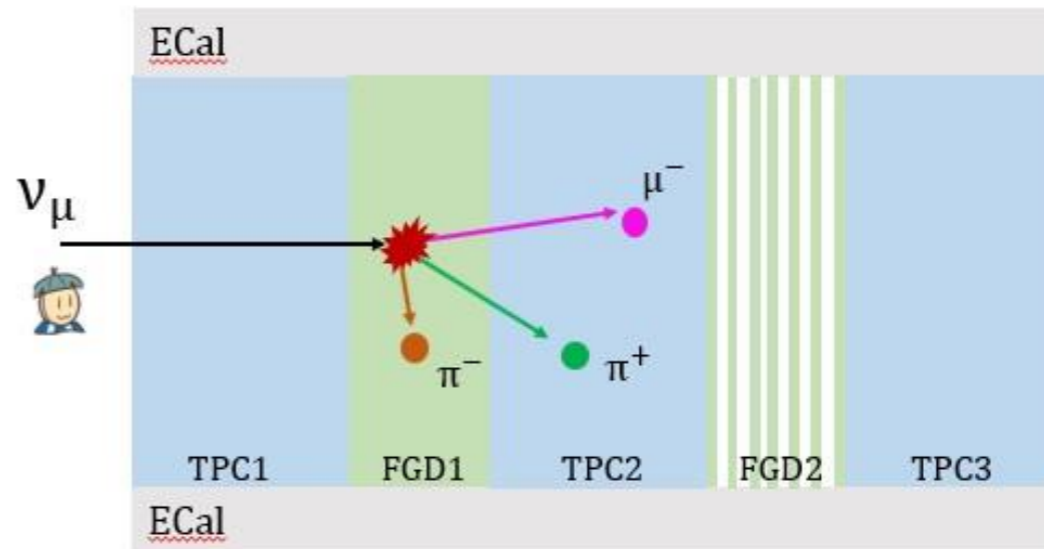
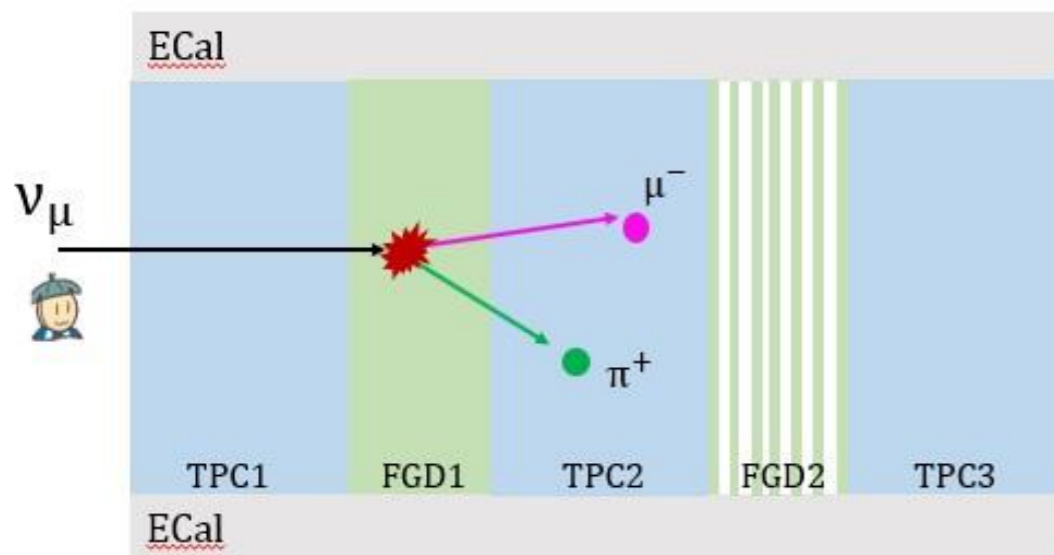
Signal:

- $CC1\pi^+$:
 - one negatively charged muon,
 - one positively charged pion,
 - no other pions,
 - any number of nucleons.

Analysis Goal: Measure the muon neutrino charged current single positive pion interaction differential cross-section using muon and pion kinematics.

Side bands or control regions:

- $CC1\pi^+1\pi^\pm$:
 - one negatively charged muon,
 - one positively charged pion,
 - one other charged pion,
 - any number of nucleons.
- $CC1\pi^+1\pi^0$:
 - one negatively charged muon,
 - one positively charged pion,
 - one other neutral pion,
 - any number of nucleons.



Analysis summary

The flux-integrated cross-section:

- experiment-dependent results since no bin-by-bin correction for the flux is applied.
- completely model-independent since no assumption needs to be made on the particular neutrino energy distribution in each kinematic bin.

of signal events in bin i

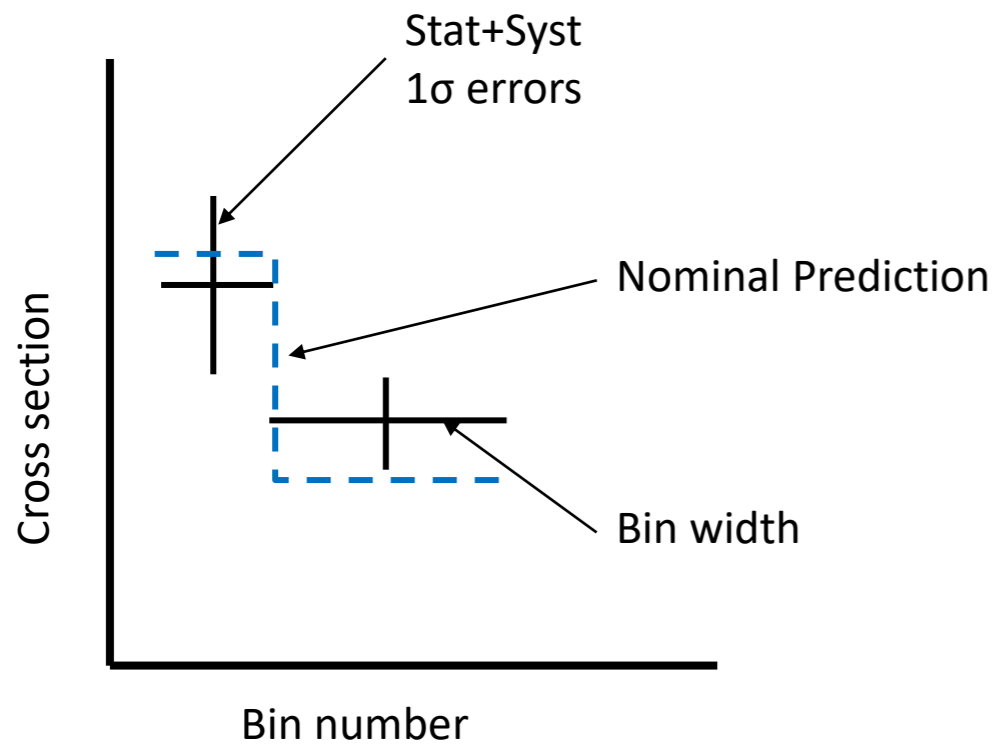
$$\left[\frac{d\sigma_{CC1\pi^+}}{dP_\mu d\cos\theta_\mu dP_{\pi^+} d\cos\theta_{\pi^+}} \right]_{\text{cm}^2/\text{nucleon}/\frac{\text{MeV}}{c}} = \frac{N_{CC1\pi^+,i}}{\epsilon_i \Phi N_{\text{target}} \Delta P_\mu \Delta \cos\theta_\mu \Delta P_{\pi^+} \Delta \cos\theta_{\pi^+}}$$

The diagram illustrates the relationship between the flux-integrated cross-section and the number of signal events in a bin. The left side shows the cross-section $d\sigma_{CC1\pi^+}$ in units of $\text{cm}^2/\text{nucleon}/\frac{\text{MeV}}{c}$, divided by the differential phase space elements $dP_\mu d\cos\theta_\mu dP_{\pi^+} d\cos\theta_{\pi^+}$. This is equal to the number of signal events $N_{CC1\pi^+,i}$ in bin i , divided by the product of detector efficiency ϵ_i , incoming neutrino flux Φ , number of target nucleons N_{target} , and the bin width $\Delta P_\mu \Delta \cos\theta_\mu \Delta P_{\pi^+} \Delta \cos\theta_{\pi^+}$.

Quadruple differential cross section

How to read!

Figure from Dr. Andrew Cudd



$\cos \theta_{\mu}$		P_{μ}		$\cos \theta_{\pi^+}$		P_{π^+}	
-1.0	0.6	200	30000	-1.0	1.0	160	30000
0.6	0.8	200	400	-1.0	1.0	160	30000
0.6	0.8	400	30000	-1.0	1.0	160	30000
0.8	0.9	200	1000	-1.0	0.7	160	30000
0.8	0.9	200	1000	0.7	1.0	160	30000
0.8	0.9	1000	30000	-1.0	1.0	160	30000
0.9	1.0	200	1000	-1.0	1.0	160	300
0.9	1.0	200	1000	-1.0	1.0	300	30000
0.9	1.0	1000	2500	-1.0	0.7	160	30000
0.9	1.0	1000	2500	0.7	1.0	160	600
0.9	1.0	1000	2500	0.7	1.0	600	30000
0.9	1.0	2500	30000	-1.0	0.7	160	30000
0.9	1.0	2500	30000	0.7	1.0	160	30000

Quadruple differential cross section

Comparing NEUT to the fake data (GENIE)

Overestimation of the cross section in bins 2 to 7 and 12:

Bin2:

$$0.6 < \cos \theta_{\mu} < 0.8$$

$$0.4 \text{ GeV} < P_{\mu} < 30 \text{ GeV}$$

Bin3+4+5:

$$0.8 < \cos \theta_{\mu} < 0.9$$

Bin6+7:

$$0.9 < \cos \theta_{\mu} < 1.0$$

$$1.0 \text{ GeV} < P_{\mu} < 30 \text{ GeV}$$

Bin12:

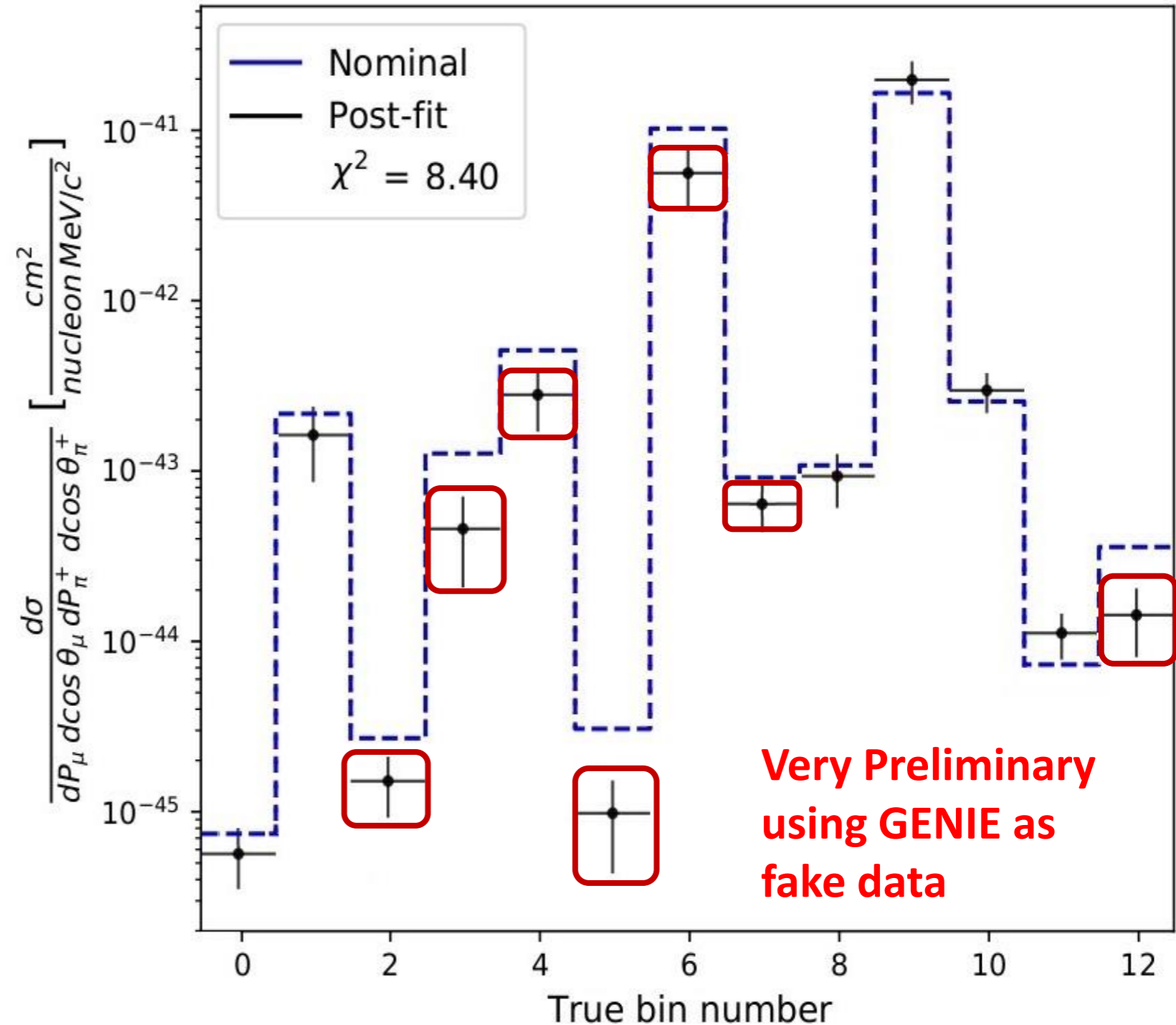
$$0.9 < \cos \theta_{\mu} < 1.0$$

$$2.5 \text{ GeV} < P_{\mu}$$

$$0.7 < \cos \theta_{\pi^+} < 1.0$$

Deficiency in our theoretical models when describing:

- RES to DIS transitions
- π absorption and production models (Rein-Sehgal)



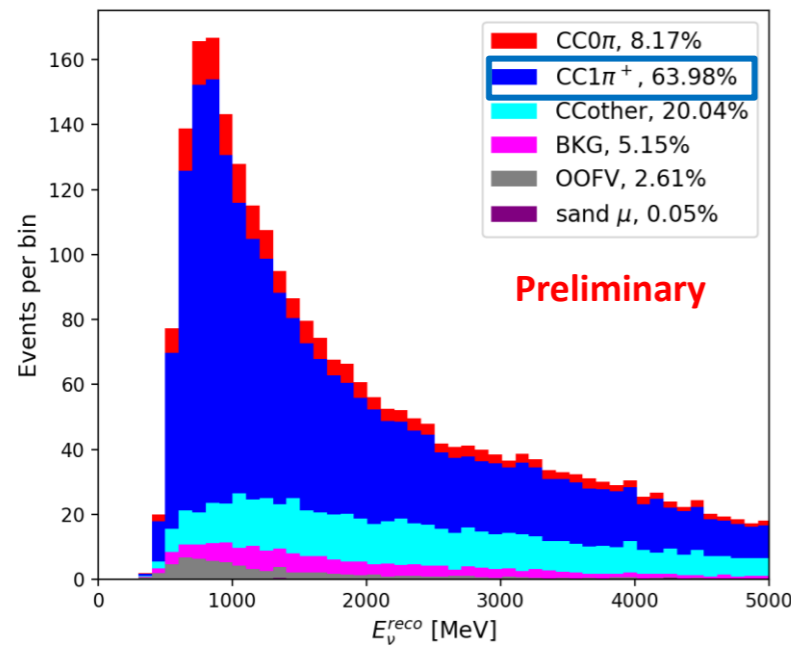
Neutrino energy, Adler angles, and asymmetry

Measuring neutrino energy

Neutrino energy is reconstructed:

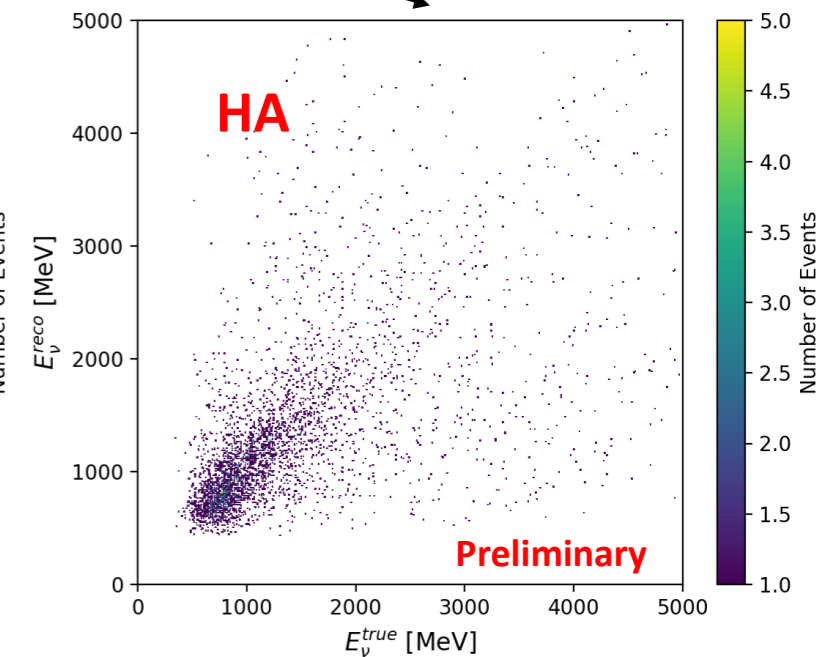
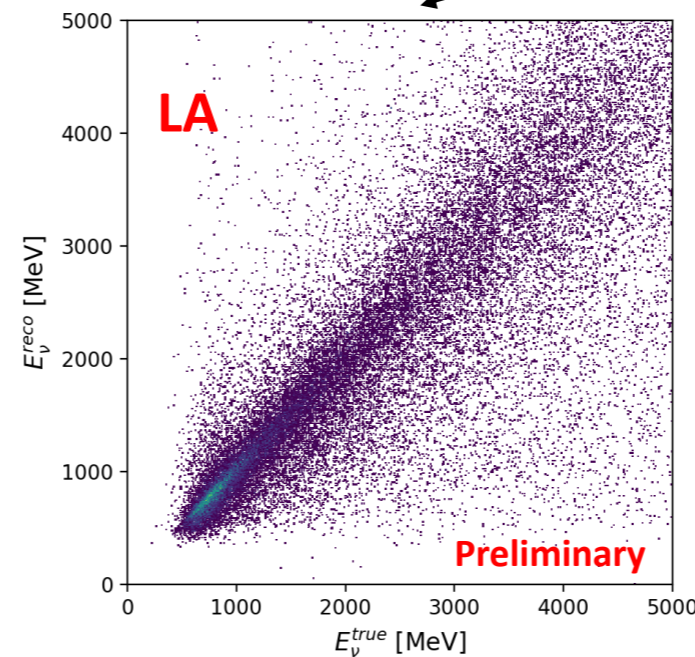
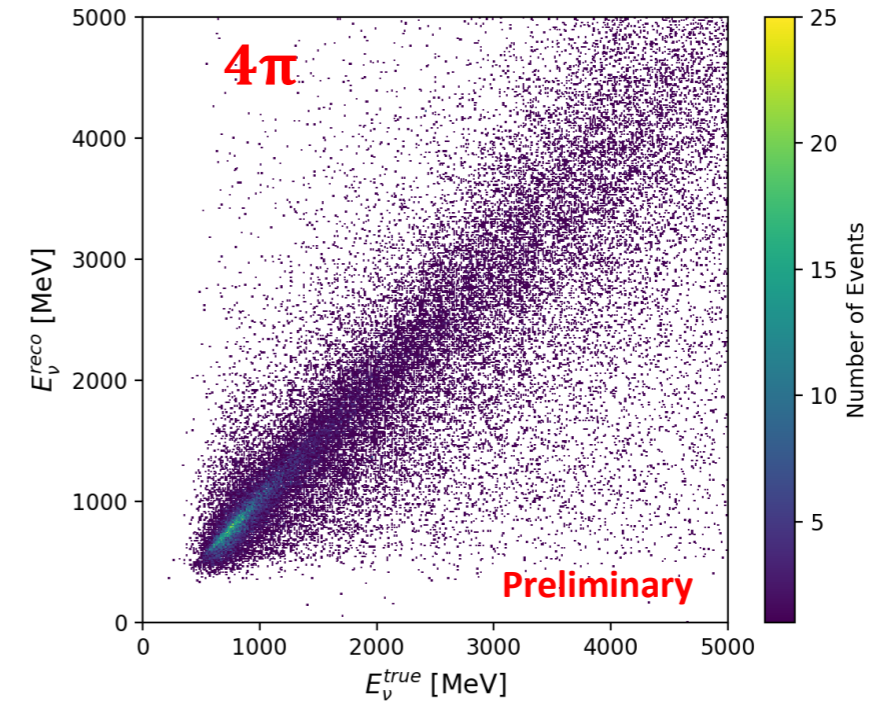
- using leptonic and hadronic kinematics,
- assuming stationary target (a nucleon),
- massless neutrino.

$$E_{\nu}^{\text{reco}} = \frac{m_p^2 - (m_p - E_{\text{bind}} - E_{\mu} - E_{\pi})^2 + |\vec{P}_{\mu} + \vec{P}_{\pi}|^2}{2\{m_p - E_{\text{bind}} - E_{\mu} - E_{\pi} + \hat{k}_{\nu}(\vec{P}_{\mu} + \vec{P}_{\pi})\}}$$



This introduce some biases:

- Due to initial state interactions (Fermi motion),
- The detector misses neutral particles,

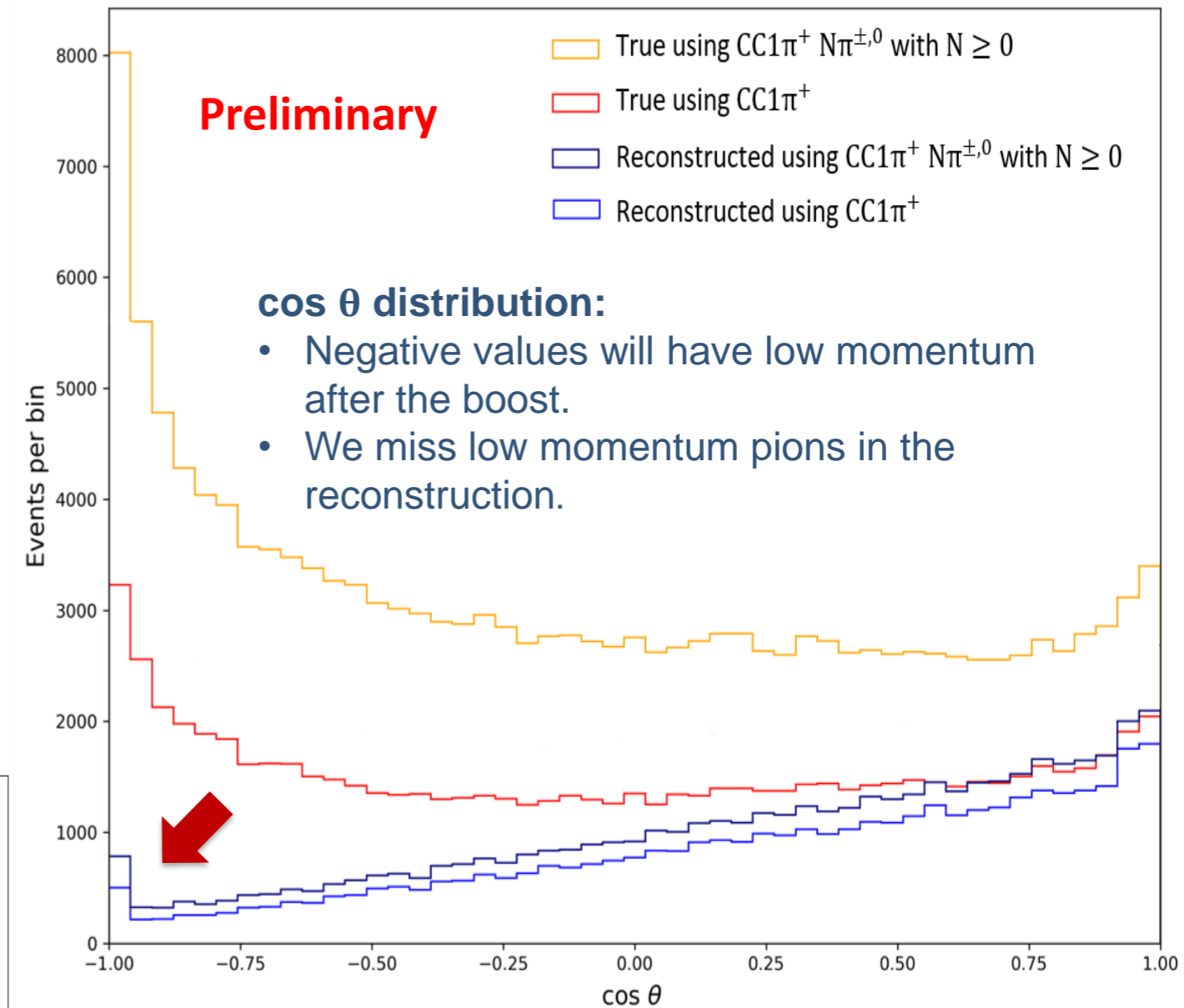
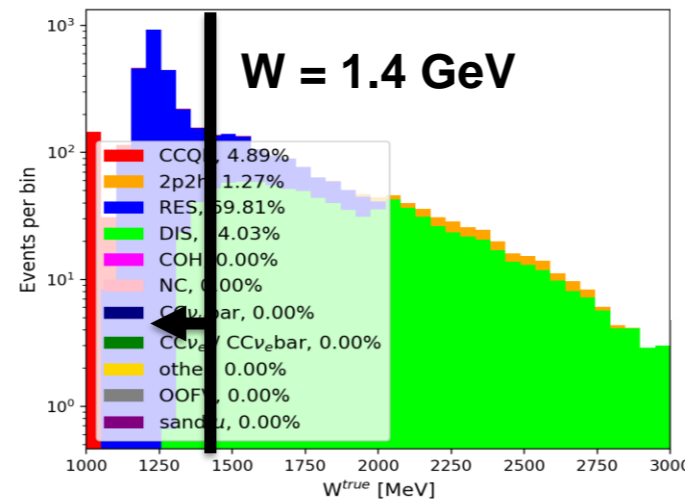
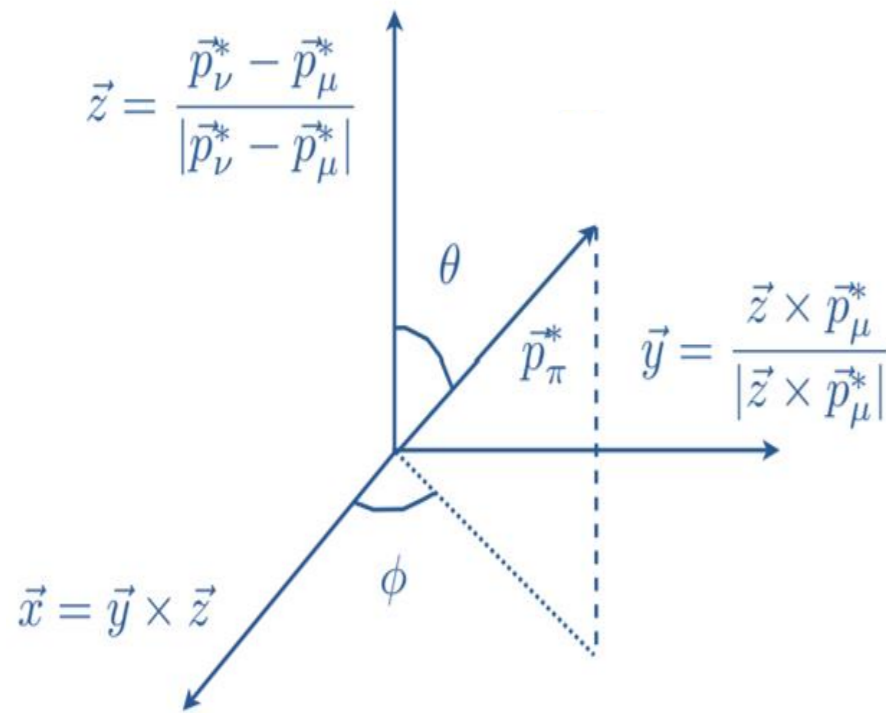


Adler angles

The angles θ and ϕ are defined in the Adler system which corresponds to the Δ (rest frame).

The Adler angles carry information about:

- the polarization of the Δ resonance
- the interference with non resonant single pion production.



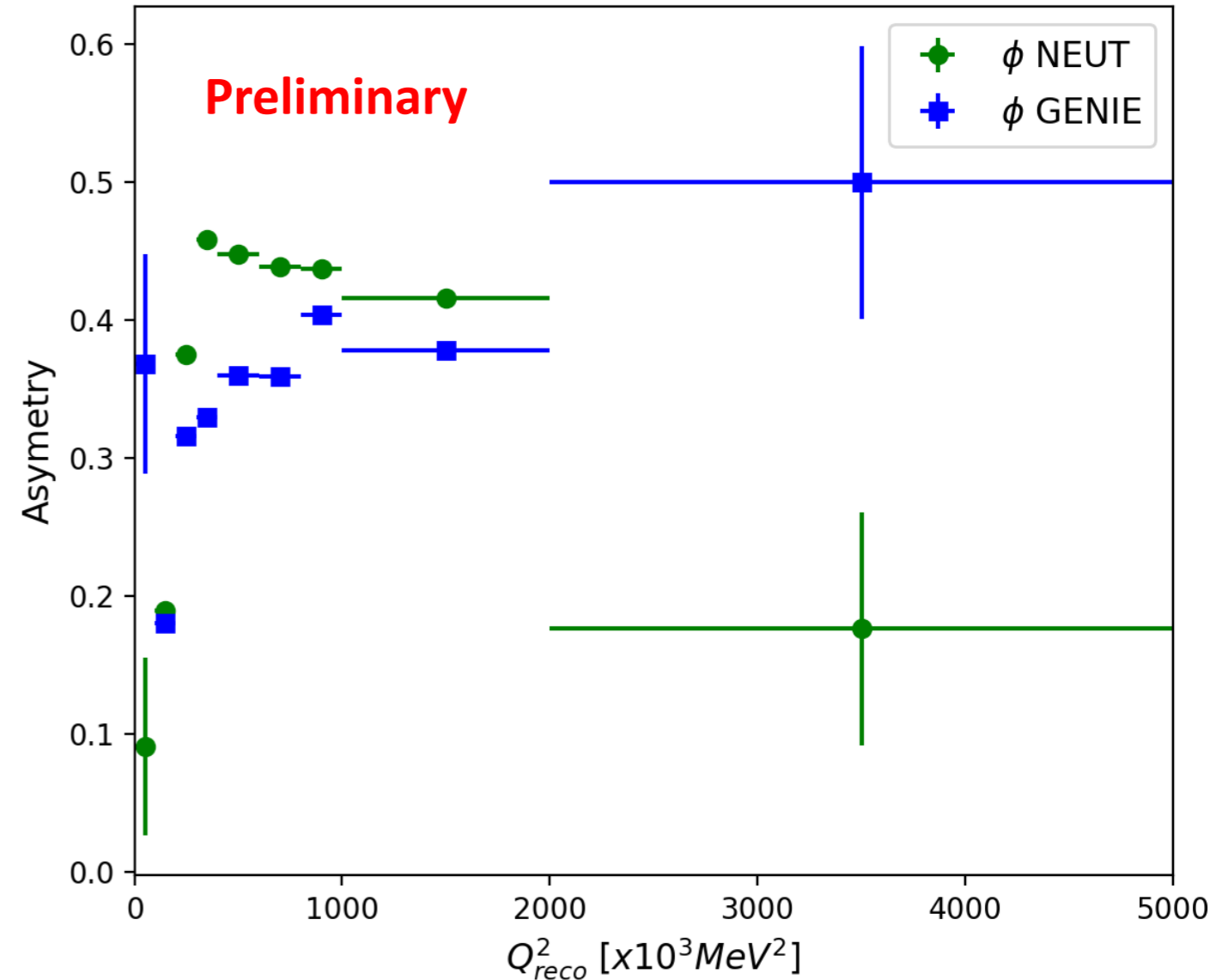
Comparison between reconstructed and true Adler angle ($\cos \theta$) distributions using in $CC1\pi^+$ or $CC1\pi^+ N\pi^{\pm,0} N \geq 0$.

Asymmetry

The FWD-BWD asymmetry of the two Adler angles with respect to the direction of the $p\pi^+$ plane:

$$\begin{cases} A_{\text{FB}}(\phi) = \frac{N_{\cos \phi > 0} - N_{\cos \phi < 0}}{N_{\cos \phi > 0} + N_{\cos \phi < 0}} \\ A_{\text{FB}}(\theta) = \frac{N_{\cos \theta > 0} - N_{\cos \theta < 0}}{N_{\cos \theta > 0} + N_{\cos \theta < 0}} \end{cases}$$

We use only ϕ (sensitive to FSI and nuclear effects) since θ is strongly dependent on the pion threshold.



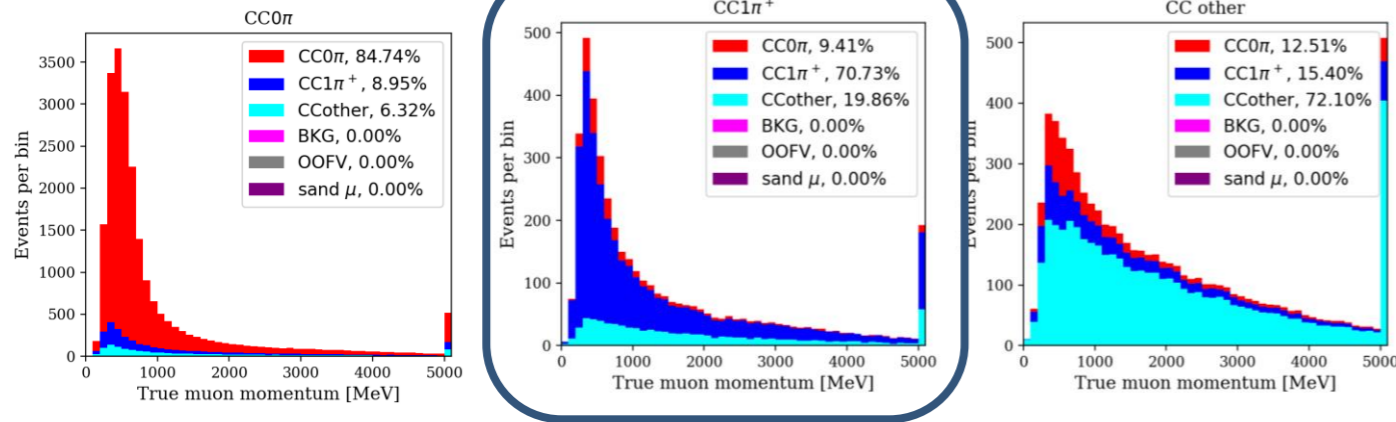
$Q^2_{\text{binning}} = [0, 100, 200, 300, 400, 600, 800, 1000, 2000, 30000]$

- The highest uncertainties were found for $Q^2 < 0.1 \text{ GeV}$ and $Q^2 > 2 \text{ GeV}$ for both NEUT and GENIE.

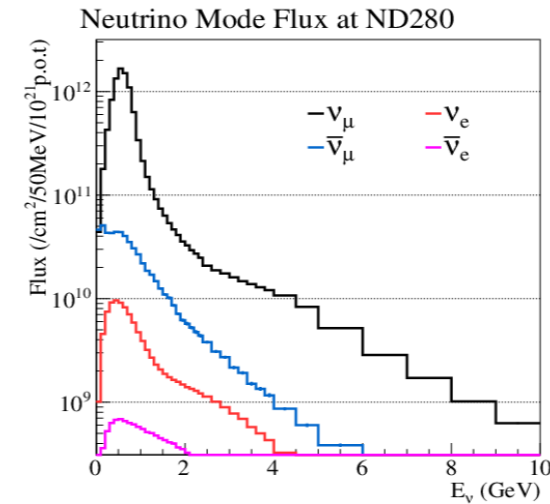
Summary and next steps

Beam And Nd280 Flux measurement task Force

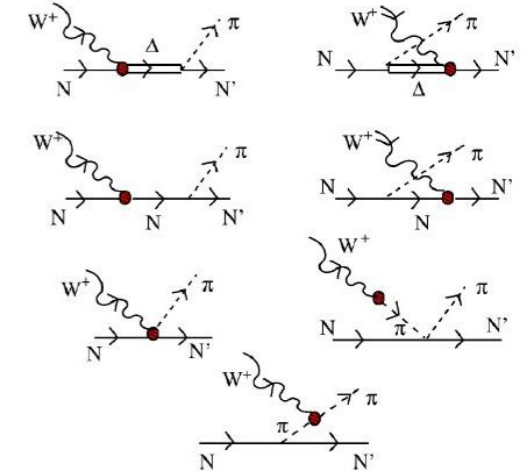
ND280 data



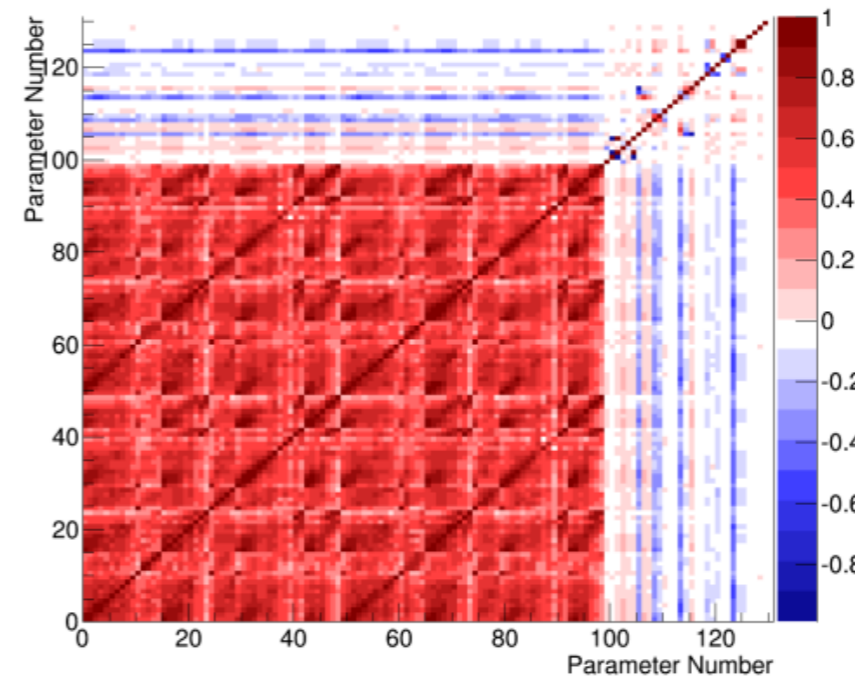
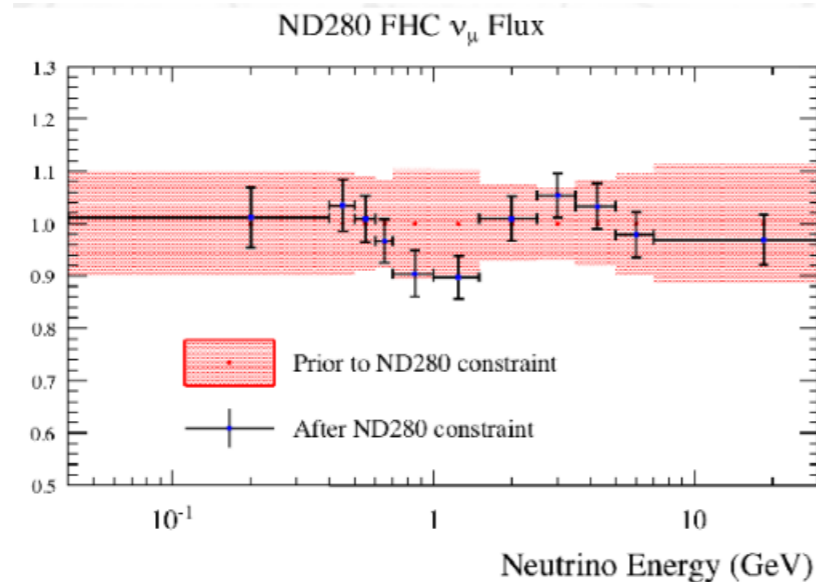
Flux prediction



Cross section model



Corrected flux and cross-section model + Covariance matrix



BANFF

Summary

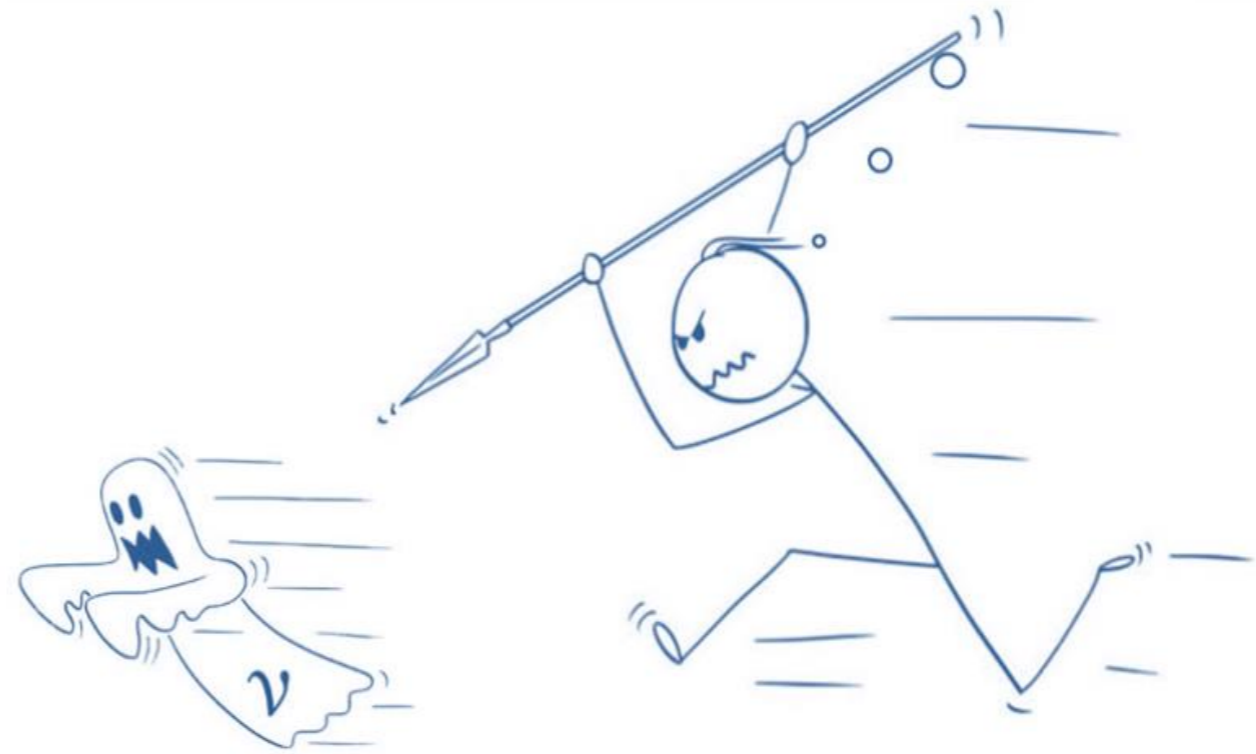
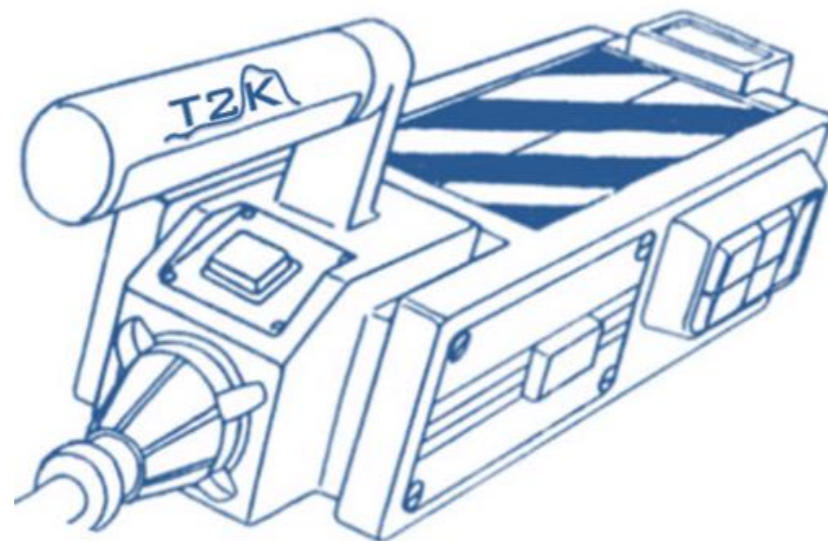
- This analysis directly addresses important challenges in the oscillation analyses.
 - interaction cross section → systematic errors are currently dominated by cross section and flux.
 - the main background for the ν_μ disappearance measurement.
 - new 2 ring signal at SK.

- This analysis will report the differential cross sections:

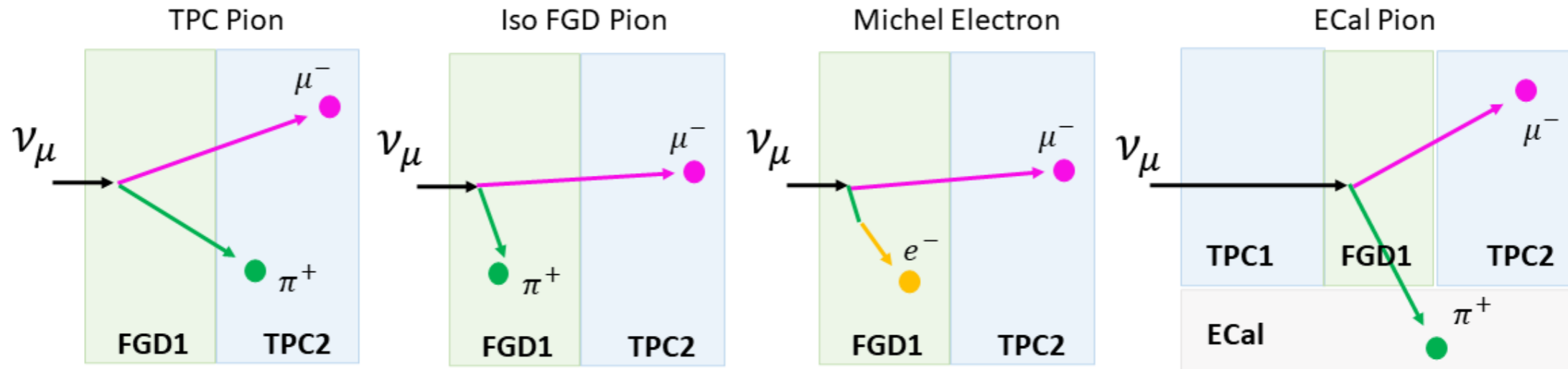
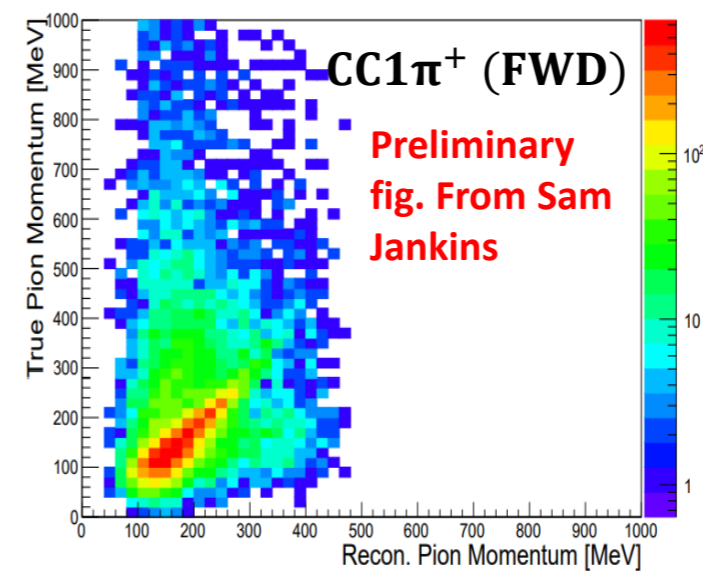
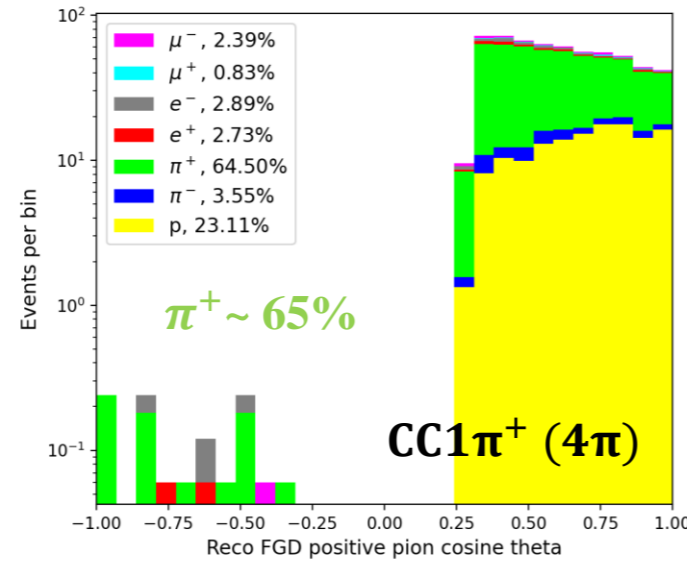
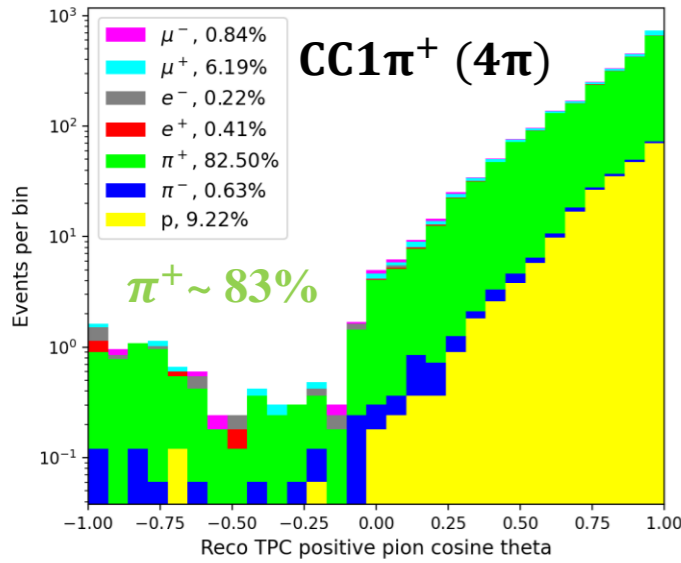
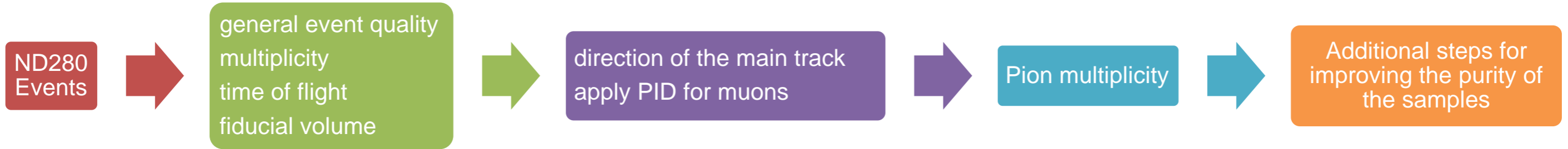
$$\frac{d\sigma}{dP_\mu d\cos\theta_\mu dP_{\pi^+} d\cos\theta_{\pi^+}}, \quad \frac{d\sigma}{dP_\mu d\cos\theta_\mu}, \quad \frac{d\sigma}{dP_{\pi^+} d\cos\theta_{\pi^+}} \quad \text{Model independent}$$

- The cross section results will allow us to evaluate our models.
- Differences in pion related models used in NEUT and GENIE, to understand the differences in the cross-section
 - Some of the variables being study are the Adler angles and their asymmetry.

Thank you very much!!!

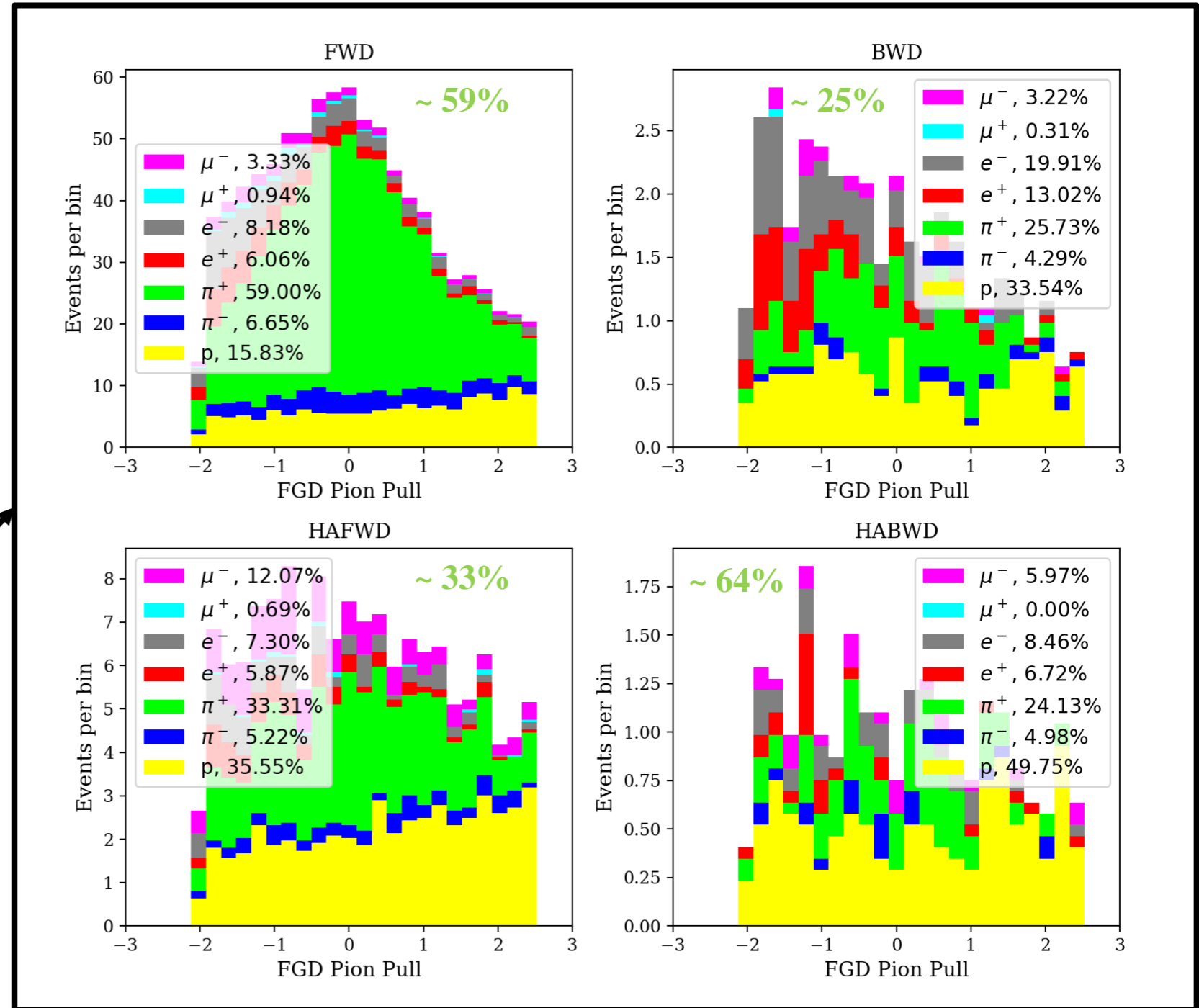
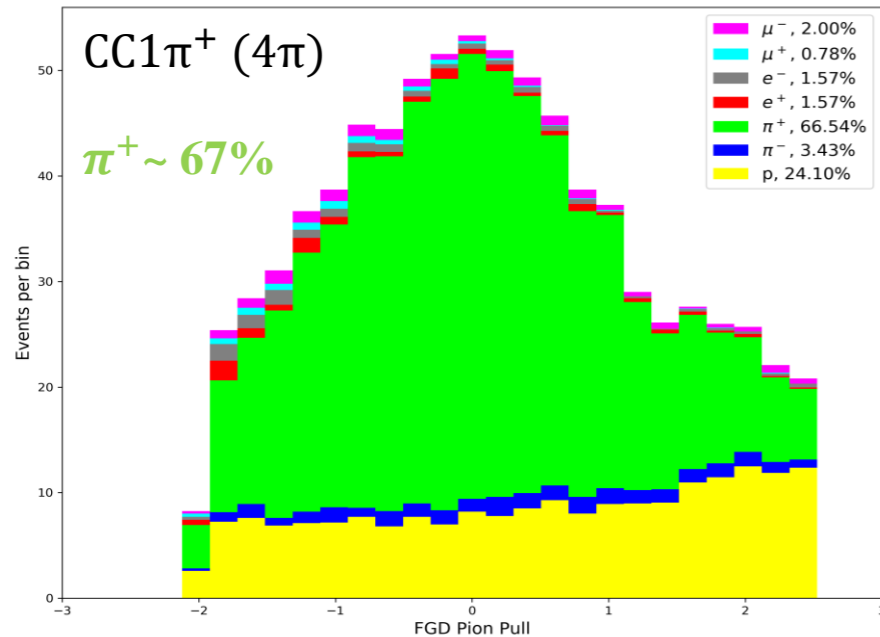
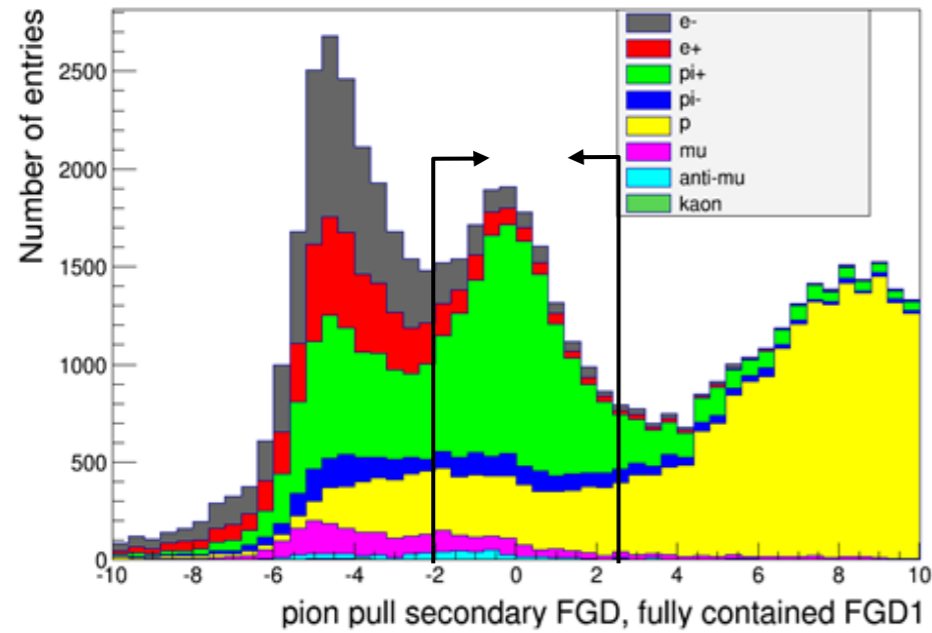


Selection steps

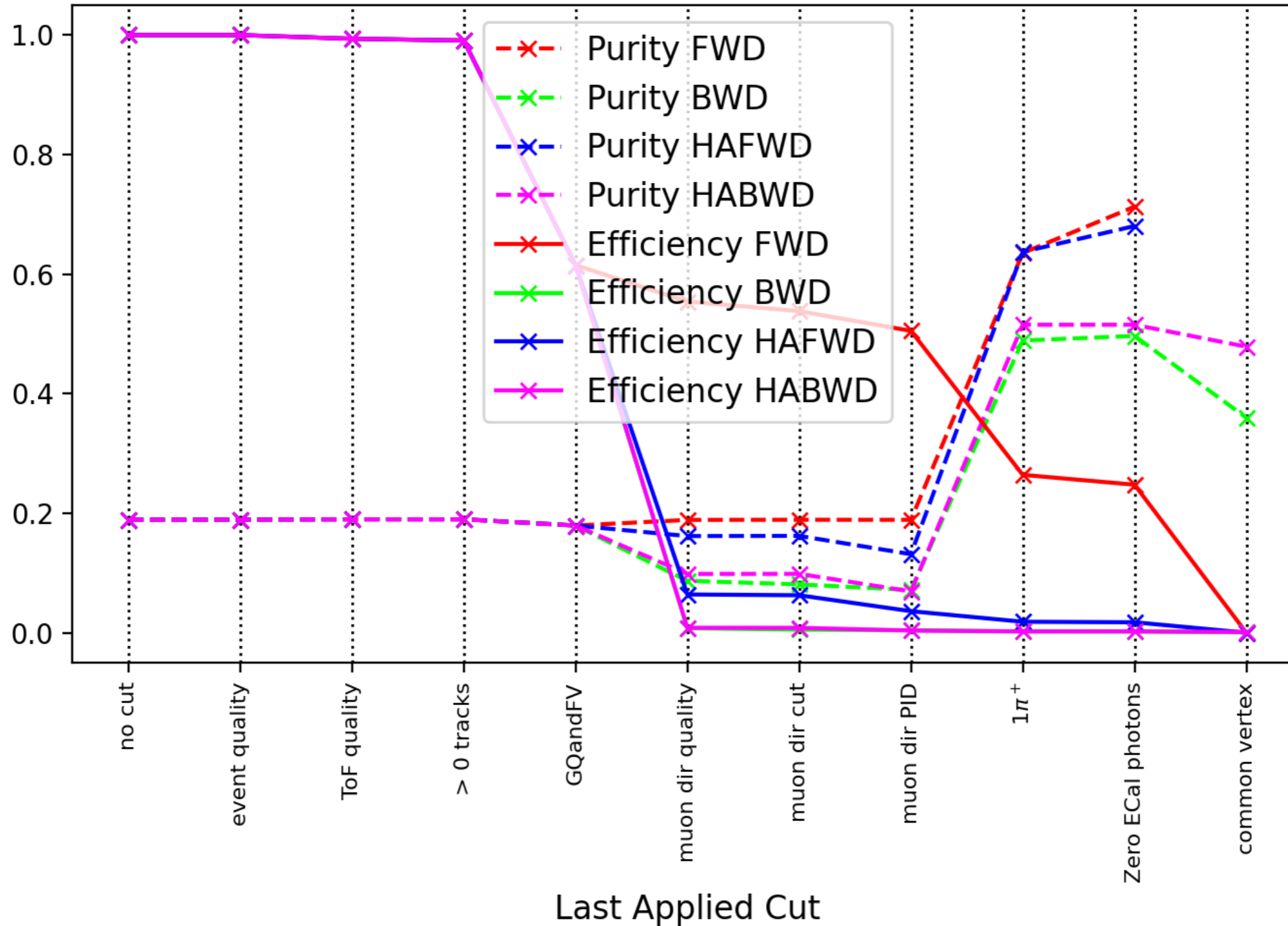


FGD pions

- A better reconstruction could improve the cut

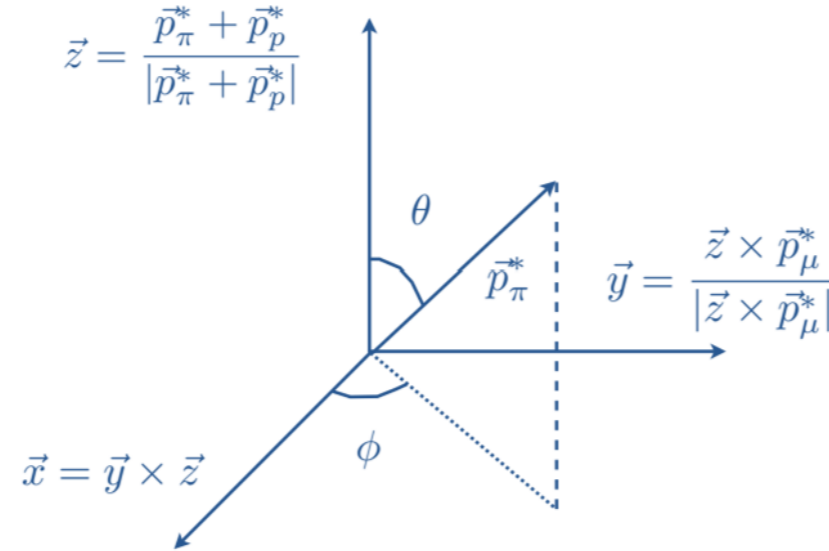
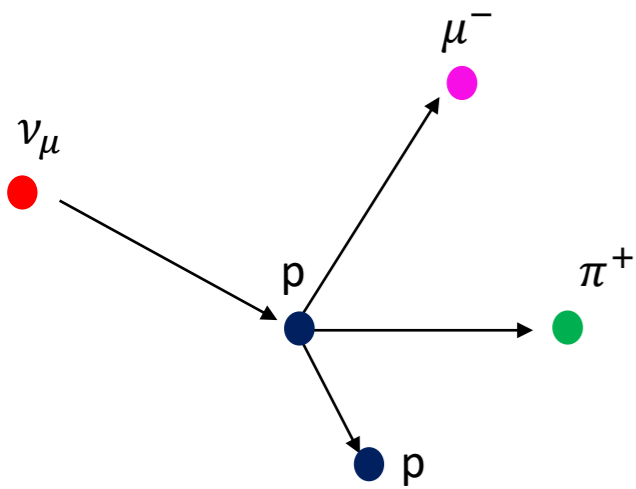


Efficiency vs. selection cut



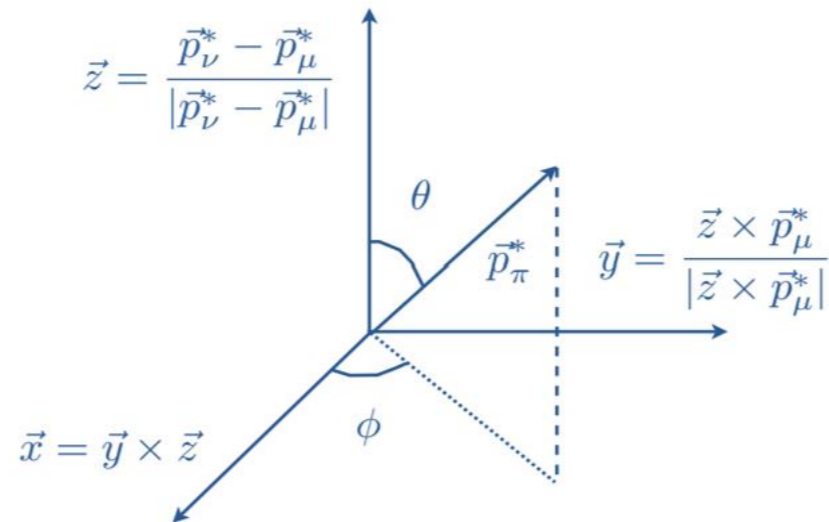
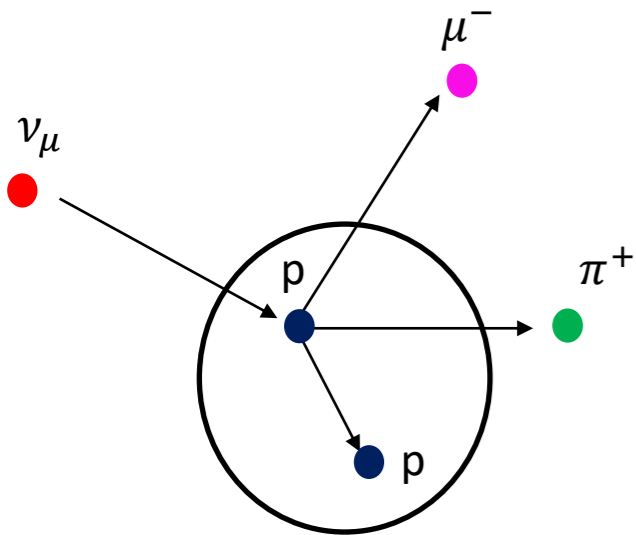
Adler angles definition

The angles θ and ϕ are defined in the Adler system which corresponds to the Δ rest frame.



Level 1: Nucleon level

- Fermi momentum effect



Level 2: Nucleus level

- Fermi momentum + FSI effects

Level 3: Reconstructed nucleus level

- Fermi momentum + FSI + nuclear medium effects

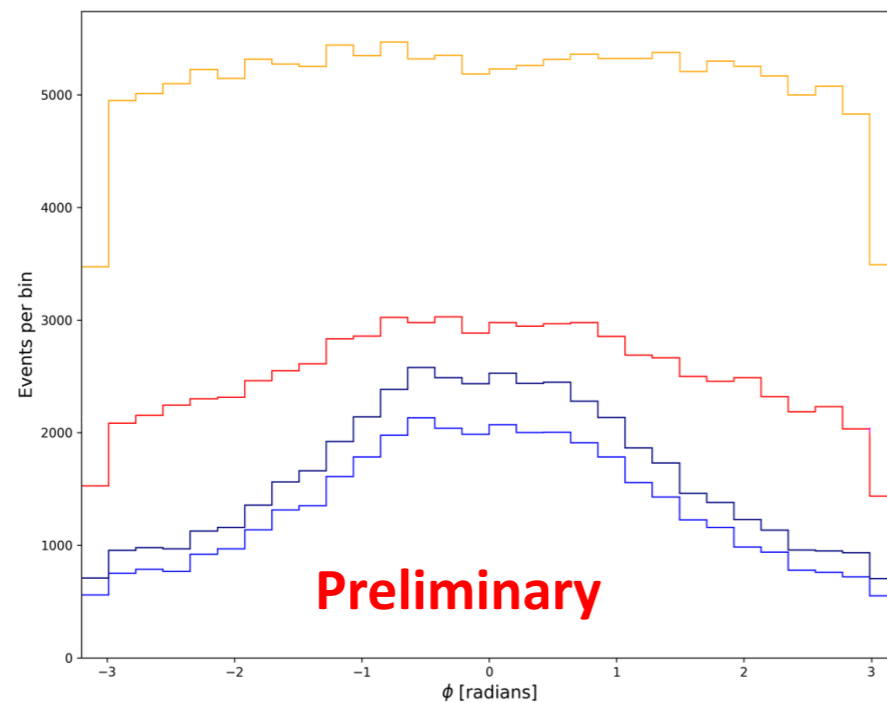
Adler angles

The Adler angles carry information about:

- the polarization of the Δ resonance
- the interference with non resonant single pion production.

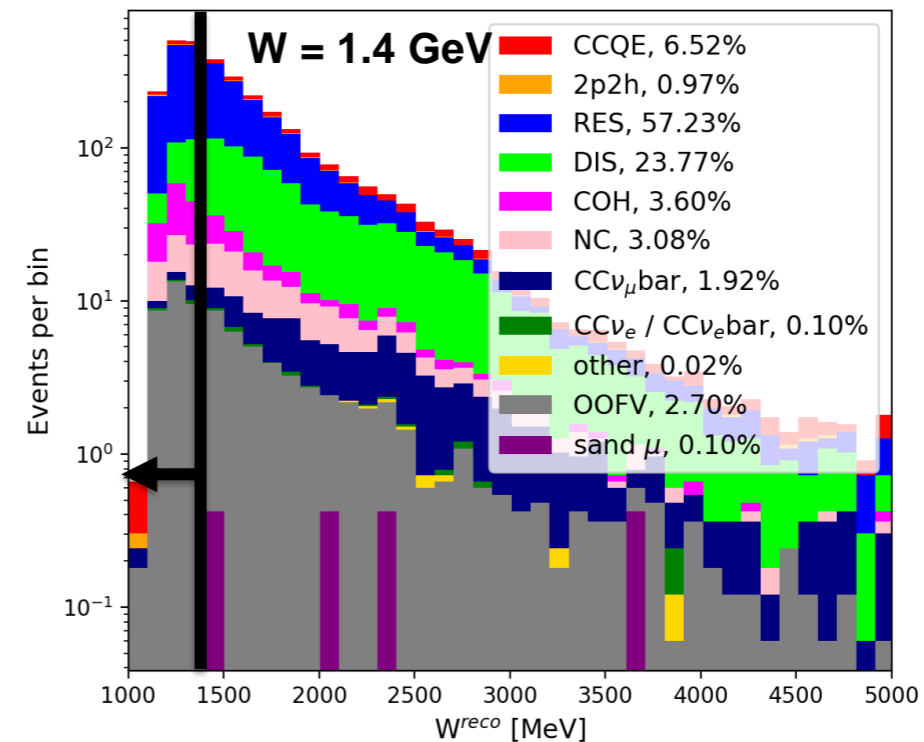
These Adler angles can allow us to study nuclear effects, FSI and Fermi momentum by computing them at different levels.

Comparison between reconstructed and true Adler angle (ϕ) distributions using in $CC1\pi^+$ or $CC1\pi^+N\pi^{\pm,0}$ $N \geq 0$.



ϕ distribution:

- it shows a peak around zero
- This is due to FSI and nuclear effects

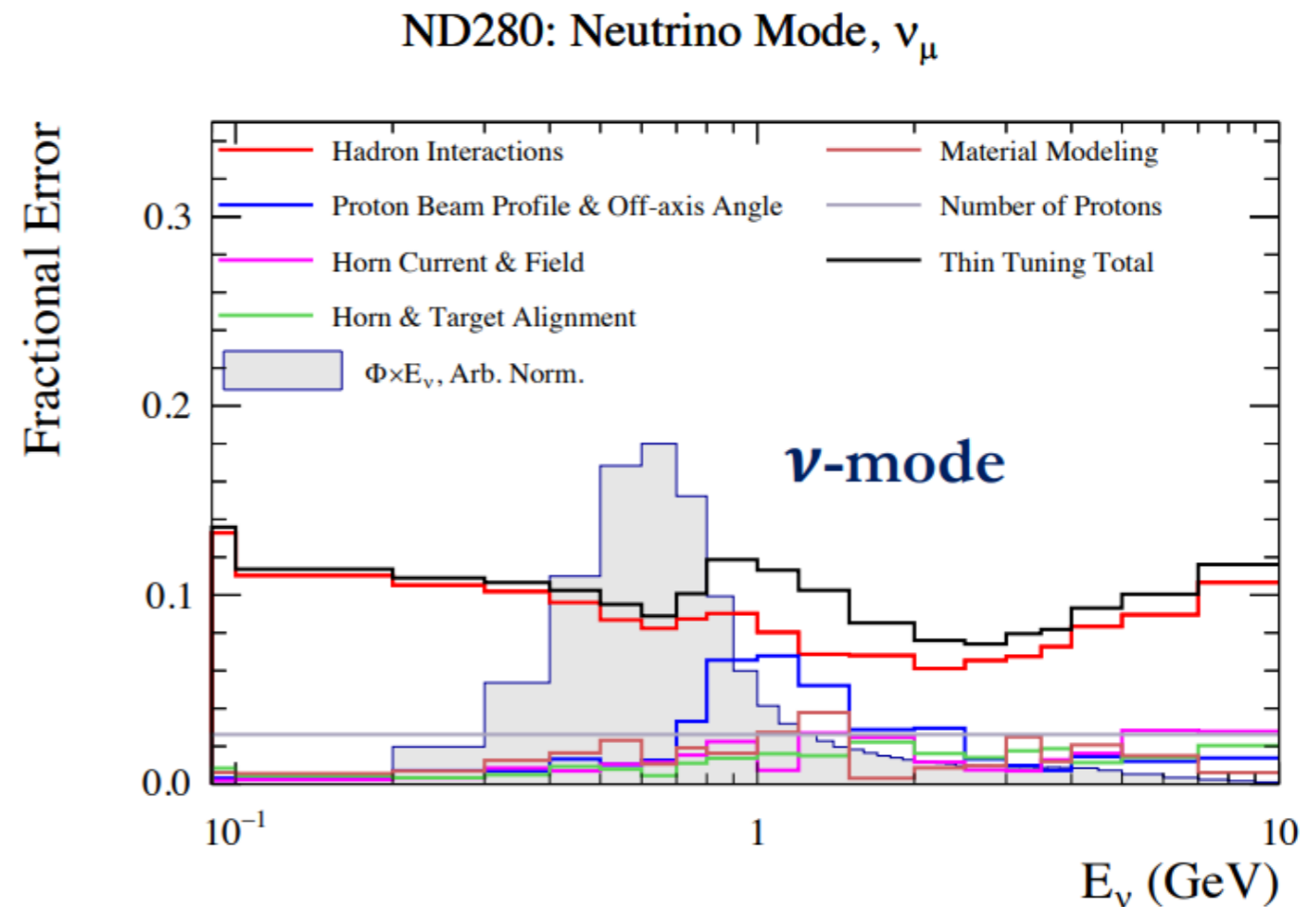


Flux model

The flux model is studied by comparisons to cross section and particle production data, and simulations of changing the characteristics of the beam and beamline.

Examples include:

- Proton--Carbon cross section
- Pion--Carbon cross section
- Horn current absolute value
- Horn alignment



Interaction model

- Based on a set of models for each neutrino interaction process, and includes nuclear effects.
- The fit includes a series of nuisance parameters which either change the underlying physics model parameters or act as a scaling on a given aspect of the interaction model.

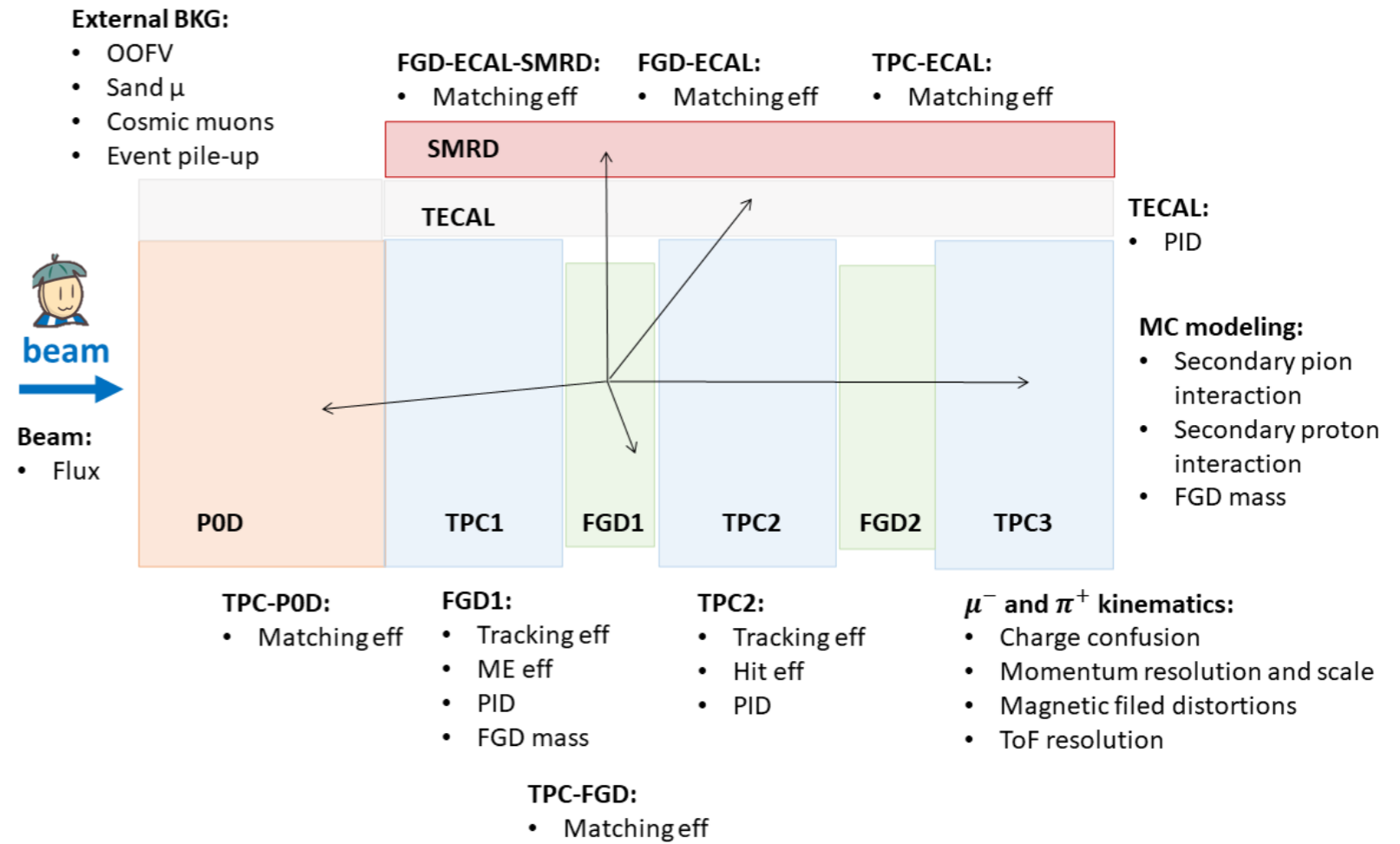
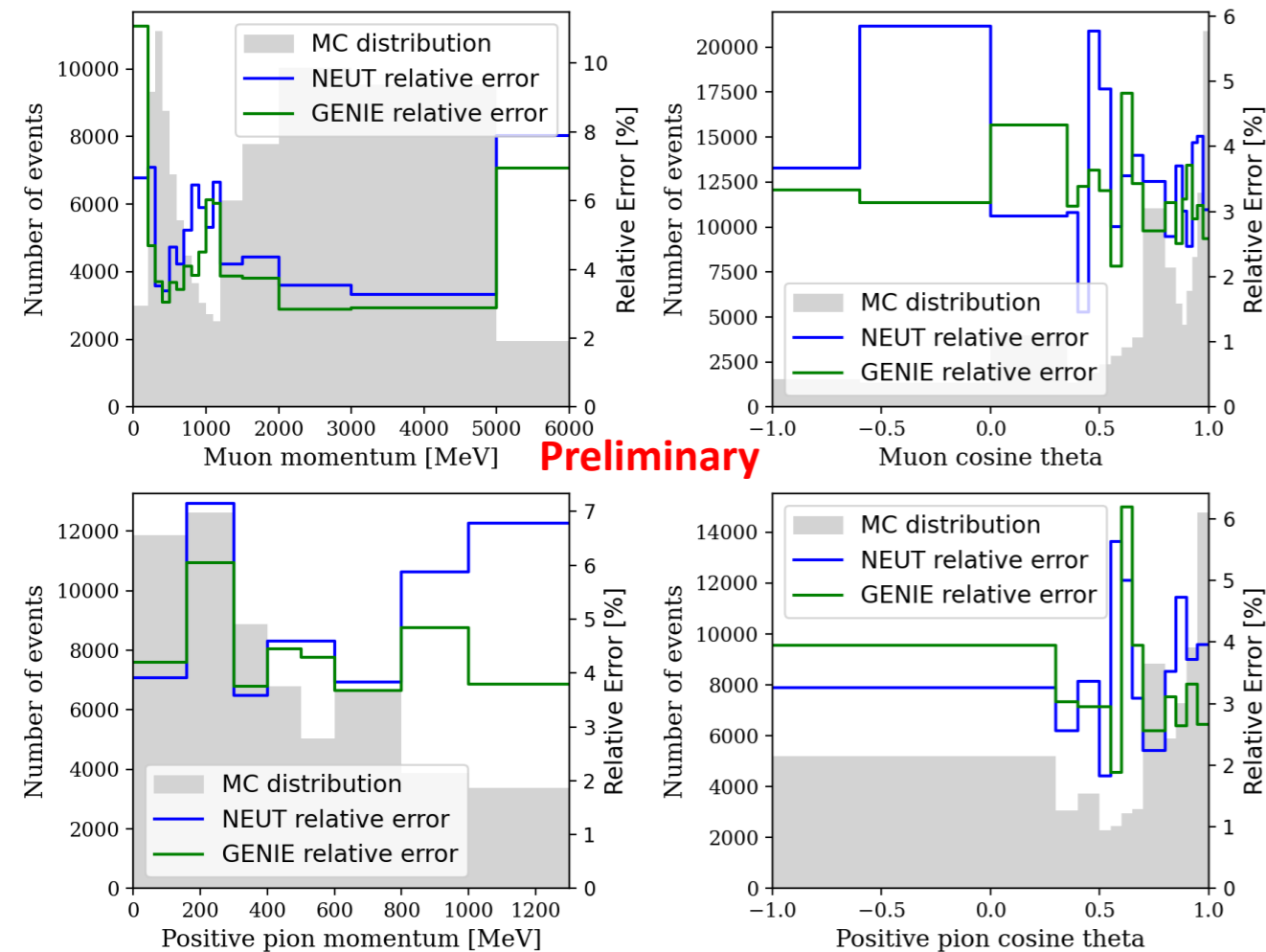
Examples include:

- Pion prod/ abs, that will affect FSI

Index	Parameter	Type	Prior	Error
0	M_A^{QE}	Signal shape	1.21	0.3
1	2p2h ν norm.	Signal normalization	1.0	1.0
2	2p2h ν shape	Signal shape	1.0	1.0
3	M_A^{Res}	Background shape	0.95	0.15
4	C_A^5	Background shape	1.01	0.12
5	$I_{1/2}$ Bkg Resonant	Background normalization	1.3	0.2
6	DIS Multiple pion	Background shape	1.0	0.4
7	CC-1 π $E_\nu < 2.5$ GeV	Background normalization	1.0	0.5
8	CC-1 π $E_\nu > 2.5$ GeV	Background normalization	1.0	0.5
9	CC DIS	Background normalization	1.0	0.5
10	CC Multi- π	Background normalization	1.0	0.5
11	CC Coherent on C	Background normalization	1.0	1.0
12	NC Coherent	Background normalization	1.0	0.3
13	NC Other	Background normalization	1.0	0.3
14	CC ν_e	Background normalization	1.0	0.03
15	FSI Inelastic, LE	Background shape	1.0	0.41
16	FSI π absorption	Background shape	1.1	0.41
17	FSI Charge exchange, LE	Background shape	1.0	0.57
18	FSI Inelastic, HE	Background shape	1.8	0.34
19	FSI π production	Background shape	1.0	0.50
20	FSI Charge exchange, HE	Background shape	1.8	0.28

Detector model

- The detector model is studied through a series of control samples to evaluate the ND280 detector performance.
- The effects of the detector uncertainties are parameterized as a function of muon and pion kinematics and included in the fit.



Analysis summary

The flux-integrated cross-section:

- experiment-dependent results since no bin-by-bin correction for the flux is applied.
- completely model-independent since no assumption needs to be made on the particular neutrino energy distribution in each kinematic bin.

of signal events in bin i

$$\left[\frac{d\sigma_{CC1\pi^+}}{dP_\mu d\cos\theta_\mu dP_{\pi^+} d\cos\theta_{\pi^+}} \right] = \frac{N_{CC1\pi^+,i}}{\epsilon_i \Phi N_{target}} \frac{1}{\Delta P_\mu \Delta \cos\theta_\mu \Delta P_{\pi^+} \Delta \cos\theta_{\pi^+}}$$

$\left[\text{cm}^2 / \text{nucleon} / \frac{\text{MeV}}{c} \right]$

Detector efficiency in bin i Incoming ν flux # of targets (nucleons) Bin i width

13 template parameters

- directly scale the cross-section
- free

20 flux parameters

20 interaction model parameters

41 detector parameters

- constrained
- prior correlations → avoid very unphysical configurations

Fake data studies

Fit name	Description
Asimov fit	data identical to MC simulation (Sec. 8.1.1).
Random template priors	Asimov fit where the prior values of the template parameters have been randomized (Sec. 8.1.2).
MC statistical fluctuations	Asimov fit with variations of truth bins according to Poisson fluctuations (Sec. 8.1.3).
Altered OOFV weights	Data fit to decreased the oofv events weights ($0.9 \cdot \text{weight}$) (Sec. 8.2.1).
Altered CCoher weights	Data fit to decreased the control sample events weights ($0.9 \cdot \text{weight}$) (Sec. 8.2.2).
Altered OOPS kinematics weights	Data fit to increased the weights ($1.1 \cdot \text{weight}$) of events with $P_\mu \leq 200 \text{ MeV}$ or $P_{\pi^+} \leq 160 \text{ MeV}$ (Sec. 8.2.3).
Altered resonant weights	Data fit to increased the resonant events weights ($1.3 \cdot \text{weight}$) (Sec. 8.2.4).
GENIE MC	Data fit to MC events generated with the GENIE neutrino interaction simulation (Sec. 8.2.5).

The fitter framework performed well in almost every validation test:

- being capable of identifying single changes.

TABLE 8.1: List of fake data studies performed to validate the analysis, with short description.